

Energy Research and Development Division  
FINAL PROJECT REPORT

**CARBON DYNAMICS AND  
GREENHOUSE GAS EMISSIONS OF  
STANDING DEAD TREES IN  
CALIFORNIA MIXED CONIFER  
FORESTS**

Prepared for: California Energy Commission  
Prepared by: University of California Berkeley



JUNE 2014  
CEC-500-2016-001

***Prepared by:***

***Primary Authors:***

John J. Battles  
Stella J.M. Cousins  
John E. Sanders

University of California Berkeley  
Department of Environmental Science, Policy, and Management  
130 Mulford Hall #3114  
Berkeley, CA 94720  
Phone: 510-643-2450

***Contract Number: 500-10-046***

***Prepared for:***

**California Energy Commission**

David Stoms  
***Project Manager***

Aleecia Gutierrez  
***Office Manager***  
***Energy Generation Research Office***

Laurie ten Hope  
***Deputy Director***  
***ENERGY RESEARCH AND DEVELOPMENT DIVISION***

Robert P. Oglesby  
***Executive Director***

**DISCLAIMER**

This report was prepared as the result of work sponsored by the California Energy Commission. It does not necessarily represent the views of the Energy Commission, its employees or the State of California. The Energy Commission, the State of California, its employees, contractors and subcontractors make no warranty, express or implied, and assume no legal liability for the information in this report; nor does any party represent that the uses of this information will not infringe upon privately owned rights. This report has not been approved or disapproved by the California Energy Commission nor has the California Energy Commission passed upon the accuracy or adequacy of the information in this report.

## **ACKNOWLEDGEMENTS**

The authors gratefully acknowledge those who assisted with sample collection and preparation: Debra Larson, David Soderberg, Eric Olliff, Alexander Javier, Natalie Holt, Clayton Sodergren, Erika Blomdahl, and Joe Battles. The authors further thank Robert York, Research Director at Blodgett Forest Research Station, for his generous contributions to site selection efforts and permission to sample trees. Thanks also to Ken Somers and Pete Zellner for their work safely choosing and felling trees. Finally, we are grateful to cooperators Adrian Das and Nathan Stephenson of the United States Geologic Survey - Western Ecological Research Station and Koren Nydick of the National Park Service for their assistance with sampling and analysis of the Forest Demography Study plots in Sequoia and Kings Canyon National Parks.

## PREFACE

The California Energy Commission Energy Research and Development Division supports public interest energy research and development that will help improve the quality of life in California by bringing environmentally safe, affordable, and reliable energy services and products to the marketplace.

The Energy Research and Development Division conducts public interest research, development, and demonstration (RD&D) projects to benefit California.

The Energy Research and Development Division strives to conduct the most promising public interest energy research by partnering with RD&D entities, including individuals, businesses, utilities, and public or private research institutions.

Energy Research and Development Division funding efforts are focused on the following RD&D program areas:

- Buildings End-Use Energy Efficiency
- Energy Innovations Small Grants
- Energy-Related Environmental Research
- Energy Systems Integration
- Environmentally Preferred Advanced Generation
- Industrial/Agricultural/Water End-Use Energy Efficiency
- Renewable Energy Technologies
- Transportation

*Carbon Dynamics and Greenhouse Gas Emissions of Standing Dead Trees in California Mixed Conifer Forests* is the final report for the *Carbon Dynamics And Greenhouse Gas Emissions From Standing Dead Trees In California Forests* project (grant number 500-10-046) conducted by the University of California Berkeley. The information from this project contributes to the Energy Research and Development Division's Energy-Related Environmental Research Program.

For more information about the Energy Research and Development Division, please visit the Energy Commission's website at [www.energy.ca.gov/research/](http://www.energy.ca.gov/research/) or contact the Energy Commission at 916-327-1551.

## ABSTRACT

Increasing climatic stress, outbreaks of pests, and chronic air pollution have contributed to a global pattern of escalating forest mortality. These trends result in an unprecedented abundance of standing dead trees, with immediate implications for the dynamics of carbon sequestration and emissions by forests. Increases in standing dead trees also represent a transformation of basic ecosystem structures and functions. This study contributed to calculating accurate forest greenhouse gas budgets by characterizing the decay and demographic processes of standing dead trees and incorporating these characteristics into regional inventories and projections of forest carbon storage. The authors used dimensional analysis to describe dead tree conditions and field studies to quantify the fall rate of standing dead trees. These results were combined with a new approach for a remotely sensed greenhouse gas assessment for California's forestlands to estimate carbon storage and emissions from trees. To project potential losses due to forest disturbance, the researchers simulated a bark beetle irruption and examined the impact on greenhouse gas budgets over ten years. The investigation found that methods that do not incorporate carbon density losses overestimate the carbon storage of standing dead trees in California mixed conifer forests by 18.8 percent. More than 90 percent of standing dead trees were expected to fall within ten years of their death, with pine species falling at rates slightly faster than firs. Results from this project directly support the California Air Resources Board to implement AB32. In addition, these results suggest that the forest sector sequesters less carbon than previously estimated in standing dead trees.

**Keywords:** biomass, carbon, decay, demography, forest inventory, emissions, fall rate, greenhouse gas inventory, mixed conifer, Sierra Nevada, snag, standing dead trees

Please use the following citation for this report:

Battles, John J., Cousins, Stella J. M., and Sanders, John E. (University of California Berkeley). 2015. *Carbon Dynamics and Greenhouse Gas Emissions of Standing Dead Trees In California Mixed Conifer Forests*. California Energy Commission. Publication number: CEC-500-2016-001.

# TABLE OF CONTENTS

Acknowledgements .....	i
PREFACE .....	ii
ABSTRACT .....	iii
TABLE OF CONTENTS.....	iv
LIST OF FIGURES .....	vii
LIST OF TABLES .....	vii
EXECUTIVE SUMMARY .....	1
Introduction .....	1
Project Purpose.....	1
Project Process and Results.....	1
Project Benefits .....	3
<b>CHAPTER 1: Overview: Forest Carbon Inventorizing and Monitoring .....</b>	<b>4</b>
1.1 Need for Forest Carbon Inventory and Monitoring.....	4
1.2 IPCC Recommended Protocols.....	4
1.3 Past and Proposed Approaches to Forest GHG Accounting in California .....	5
1.4 Gaps in Assessment of Standing Dead Tree Carbon.....	5
1.4.1 Biological Gaps.....	5
1.4.2 California Challenge .....	6
1.4.3 National Challenge .....	7
1.5 Overview of this Project .....	8
1.5.1 Measure the Carbon Density in Standing Dead Trees in California Mixed Conifer Forests .....	8
1.5.2 Quantify the Fall Rates of Standing Dead Trees in the California Mixed Conifer Forests .....	8
1.5.3 Enhance Current Methods to Assess Gain-Loss of Carbon from Standing Dead Trees in California’s Conifer Forests .....	8
<b>CHAPTER 2: Carbon Density of Standing Dead Trees in California Conifer Forests.....</b>	<b>10</b>
2.1 Introduction .....	10

2.1.1	Background .....	10
2.1.2	Problem Statement: Current Approaches for Biomass Estimates in SDT .....	11
2.1.3	Carbon Density Study Objectives .....	11
<b>2.2</b>	<b>Methods .....</b>	<b>12</b>
2.2.1	Site Descriptions.....	12
2.2.2	Sampling Regime .....	13
2.2.3	Allometric Scaling.....	17
2.2.4	Whole Tree Biomass, Density Reduction Factors and Carbon Density .....	18
2.2.5	Analysis.....	18
<b>2.3</b>	<b>Results.....</b>	<b>18</b>
2.3.1	Volume and Wood Density Loss .....	18
2.3.2	Carbon Concentration and Total Carbon Biomass as a Function of Species and Decay Class .....	20
2.3.3	Bark Decay Patterns and Effect on Whole Tree Biomass .....	21
2.3.4	Net Change in Biomass and Carbon Stored.....	22
<b>2.4</b>	<b>Discussion .....</b>	<b>23</b>
2.4.1	Patterns in Biomass Loss.....	23
2.4.2	Attribution of Carbon Loss: Volume Loss vs. Decay .....	24
2.4.3	Evaluation of Uncertainty.....	24
<b>CHAPTER 3: Fall Rates of Standing Dead Trees in California Mixed Conifer Forests .....</b>		<b>27</b>
<b>3.1</b>	<b>Introduction .....</b>	<b>27</b>
<b>3.2</b>	<b>Methods .....</b>	<b>28</b>
3.2.1	Site Descriptions.....	28
3.2.2	Standing Dead Inventories .....	29
3.2.3	Standing Dead Tree Fall Rate Analysis.....	31
3.2.4	Incorporating Existing SDT Information.....	32
<b>3.3</b>	<b>Results.....</b>	<b>32</b>
3.3.1	Shape and Magnitude of the Fall Rate Curve .....	32
3.3.2	Survival Rates of Standing Dead Trees by Species and Size Class .....	33

3.3.3	A Comparison of SDT Fall Rates for California Mixed Conifer Tree Species .....	41
3.4	<b>Discussion</b> .....	<b>42</b>
<b>CHAPTER 4: Improving California’s Greenhouse Gas Accounting for Forest and Rangelands: Tracking Gains and Losses in the Standing Tree Carbon Pool .....</b>		<b>44</b>
4.1	<b>Introduction</b> .....	<b>44</b>
4.1.1	Background .....	44
4.1.2	Problem Statement .....	46
4.2	<b>Methods</b> .....	<b>46</b>
4.2.1	Developing GHG Accounting Approach .....	46
4.2.2	Estimating Standing Dead Tree Carbon .....	47
4.2.3	Incorporation of Revised Estimate (Chapter 2) of Standing Dead Tree Carbon Pools ..	49
4.2.4	Analytical Framework for Projecting Carbon Dynamics of Dead Trees.....	50
4.3	<b>Results</b> .....	<b>50</b>
4.3.1	Performance of LANDFIRE to Detect Changes in Standing Dead Tree Biomass.....	50
4.3.2	Performance of FIA in Estimating Standing Dead Tree Carbon .....	51
4.3.3	Impact of Improvements on Carbon Stocks and GHG Estimates.....	53
4.3.4	Five and Ten-Year Projections of SDT Carbon Storage .....	53
4.4	<b>Discussion</b> .....	<b>54</b>
4.4.1	Implications of Dead Tree Assessment Strategies to GHG Accounting .....	54
4.4.2	Implications of Dead Tree Assessment to GHG Accounting Under Scenarios of Increasing Tree Mortality.....	55
<b>CHAPTER 5: Conclusions</b> .....		<b>56</b>
5.1	<b>Contributions of Project to Carbon Science and Ecosystem Ecology</b> .....	<b>56</b>
5.2	<b>Impact of Enhancements on Current GHG Monitoring in California</b> .....	<b>56</b>
5.3	<b>Future Directions and Next Steps</b> .....	<b>57</b>
5.3.1	Rationale for Efforts to Enhance Understanding of Dead Tree Carbon Ecology.....	57
5.3.2	Limitations of LANDFIRE .....	58
5.3.3	Immediate Next Steps .....	58
5.3.4	Promise of LandTrendr: A Novel Technology Designed to Detect Forest Disturbance	58

<b>5.4 Benefits to California .....</b>	<b>59</b>
<b>GLOSSARY .....</b>	<b>60</b>
<b>REFERENCES .....</b>	<b>62</b>

## LIST OF FIGURES

Figure 1: Current standing dead and dying trees, Sequoia National Park.....	6
Figure 2: Forest Inventory and Analysis Decay Class Framework.....	14
Figure 3: Technique for Dimensional Analysis; Sampling and Measuring Volume of Decayed Wood.....	16
Figure 4. Density (g cm <sup>-3</sup> ) of Decay Classes 1-5 by Tree Taxonomic Group.....	20
Figure 5: Carbon Concentration of Decay Classes 1-5 by Tree Taxonomic Group.....	21
Figure 6: Standing Dead Tree Carbon Concentration, Density (DRF), and Net Carbon Density Relative to Live Trees for Each Decay Class .....	23
Figure 7: Standing Dead Tree Fall Rate Curves for Two Longitudinal Studies in California.....	35
Figure 8: Standing Dead Tree Fall Rate Curves for Three Common Species in Mixed Conifer Forests (white fir, ponderosa pine, sugar pine) .....	36
Figure 9. Standing dead tree fall rate curves for incense cedar, Douglas-fir, and black oak trees at BFRS.....	37
Figure 10: Standing Dead Tree Fall Rate Curves for White Fir, Ponderosa Pine, and Sugar Pine Trees at SEKI.....	38
Figure 12: Standing Dead Tree Fall Rate Curves for Red Fir and Jeffrey Pine Trees at SEKI .....	40
Figure 13: Distribution of Standing Dead Tree Annual Fall Rates for Pine Species in the Montane Forests of the Western United States (n = 31).....	42
Figure 14: Standing Dead Tree Aboveground Biomass in the Mixed Conifer Forests as a Function of Canopy Cover Class and Height Class for the California Mixed Conifer Forest .....	51
Figure 15: Relationship Between Aboveground Standing Dead Tree Carbon Density and Aboveground Live Tree Carbon Density for the 766 FIA Plots .....	52
Figure 16: Magnitude of the Overestimate in Aboveground Standing Dead Tree Carbon Density as a Function of Canopy Cover and Height Class for the California Mixed Conifer Forest.....	52
Figure 17: Decline in the Standing Dead Tree Carbon Pool Following a Simulated Beetle-Attack on Pine Trees in the California Mixed Conifer Forest .....	54

## LIST OF TABLES

Table 1: Standing Dead Tree Characteristics by Species, Decay Class, and Diameter Class .....	19
Table 2: Mean Combined Standing Dead wood and Bark Density and Dead:Live Density Ratio for Each Decay Class.....	19
Table 3: Mean Combined Standing Dead Wood and Bark Carbon Concentration and Dead:Live Carbon Concentration Ratio for Each Decay Class .....	21
Table 4: Wood Characteristics: Mean Standing Dead: Live Density Ratio and Mean Carbon Concentration for Each Decay Class .....	22
Table 5: Bark Characteristics: Mean Standing Dead:Live Density Ratio and Mean Carbon Concentration for Each Decay Class .....	22
Table 6: After Density Losses and Carbon Gains, Mean Dead:Live Net Carbon Ratio of Combined Wood and Bark for Each Decay Class .....	23
Table 7: Properties of Standing Dead Trees (wood and bark combined) for All Species and Decay Classes Sampled .....	25
Table 8: Standing Dead Wood Properties and Bark Properties for All Species and Decay Classes Sampled .....	26
Table 9: Description of Sites/Data from California Conifer Forests Used in This Report.....	29
Table 10: Standing Dead Tree Fall Rates for Blodgett Forest Research Station.....	30
Table 11: Standing Dead Tree Fall Rates for Sequoia-Kings Canyon National Parks.....	31
Table 12: Standing Dead Tree Fall Rates for Sequoia-Kings Canyon National Parks.....	34
Table 13: Comparison of Standing Dead Tree Fall Rates for Pine and True Fir Species in Four California Forests .....	41
Table 14: Summary of Major Remote Sensing Technologies Used for Assessing Carbon Stocks	45

# EXECUTIVE SUMMARY

## Introduction

About half of a tree's mass is made of carbon. As trees grow, they take in carbon dioxide from the air and convert it into leaves, bark, stem, and roots. As they die and decay, that carbon is released back into the atmosphere as carbon dioxide, a greenhouse gas. Tree death and decline are natural ecosystem processes, but forest mortality rates have recently accelerated and are continuing to climb well above historic levels. Both in California's forests and worldwide, increasing climatic stress, outbreaks of pests, and chronic air pollution have contributed to catastrophic forest die-offs. Dead trees are now a more important component of forest stands than before, and in the future their roles will be further pronounced.

These trends of dying trees have broad implications for the dynamics of forest carbon storage and greenhouse gas emissions, and therefore for California's climate strategy. This strategy relies heavily on healthy forests to remove carbon dioxide emissions from energy, transportation, and other sectors. With increasing numbers of trees dying, the scales could be tipped so that forests release more carbon than they absorb. California regulators need accurate greenhouse gas accounting to predict the capacity of California forests to store and sequester carbon. However, there are gaps in knowledge about some of the details of these processes. For instance, it is unknown how fast different species of trees decompose. Furthermore, there is no good estimate of the greenhouse gas emissions due to landscape-scale disturbance and resulting mortality, such as a widespread beetle kill. This important challenge must be addressed to inform California's climate strategy, including the amount of carbon offsets available to energy utility operators.

## Project Purpose

The California Air Resources Board inventories and regulates greenhouse gas from forests and rangelands, including those from dead trees, through the Global Warming Solutions Act, Assembly Bill 32. Meaningful, accurate greenhouse gas budgets are necessary to predict the capacity of California forests to store and sequester carbon; this directly relates to decisions about the amount of carbon offsets that energy utility operators can purchase or the amount of greenhouse gas emissions that they will have to reduce by other means. To further refine forest carbon accounting methods, this project:

- Measured the carbon density of standing dead trees in California's mixed conifer forests,
- Quantified how long it takes for standing dead trees in California's mixed conifer forests to fall to the ground, and
- Used this data to improve estimates of carbon and greenhouse gas emissions from standing dead trees, evaluate remote sensing products that inform these estimates, and assess the expected emissions from a pest-driven forest disturbance.

## Project Process and Results

This investigation of the carbon dynamics and greenhouse gas emissions of standing dead trees focused on California's mixed conifer forests, the most extensive forest type in the state. Mixed

conifer forests dominate the Sierra Nevada range and occupy 5.3 percent of California's total land area (21,500 km<sup>2</sup>). Research sites included Blodgett Forest Research Station and the US Geological Survey Forest Demography plot network in Sequoia, Kings Canyon, and Yosemite National Parks. The study also incorporated standing dead tree data from previous studies in the region. The authors intentionally used the same decay classification used by the US Forest Service's Forest Inventory and Analysis program, since many large-scale greenhouse gas assessments rely on it. This classification divides tree decay into five stages.

The study characterized the density, carbon concentration, and net carbon density of trees from each of five structural stages of decay. As decay advanced, trees showed both a progressively lower density and a small increase in carbon concentration. Some variation in these patterns was evident among different species and sizes. The net result for total standing dead tree carbon density was also a decline, with carbon density in the most decayed trees only 60 percent that of live trees. This is the first measurement of standing dead tree decay patterns in mixed conifer species and the first time all five stages of decay have been measured.

The longevity of standing dead trees in mixed conifer and pine forests was also examined. This information is essential to describe the timing of carbon storage and emissions. For standing dead trees about 16 inches in diameter, half of them fell within 10.1 years at Sequoia-Kings Canyon National Parks and 4.7 years at Blodgett Forest Research Station. Firs fell more rapidly than pines overall. Larger diameter dead trees generally remained standing longer than smaller ones.

To apply carbon density loss and treefall patterns information, the improved estimates of standing dead carbon were combined in a new framework for repeatable forest sector greenhouse gas inventory. The carbon stored in standing dead trees is systematically overestimated by current methods that do not correct for decay. When estimates correct for decay, standing dead trees represent 8 percent of aboveground live carbon. Using these same methods statewide that do not account for changing carbon density results in an 18.8 percent overestimate of carbon in standing dead trees.

The study evaluated the land use/land cover products and vegetation inventories available to track biomass changes regarding their capacity to describe and track episodes of forest die-off. Existing vegetation height, a metric of the remotely sensed LANDFIRE dataset, proved best for predicting standing dead tree biomass. For forests, standing dead tree biomass significantly increased with increasing existing vegetation height. The study also projected the carbon outcomes of a major (35 percent) die-off event in the California mixed conifer forest, as might occur following a bark beetle irruption. Most of dead trees fell to the forest floor within the first five years. After ten years, only 8 percent of the original forest carbon remained in standing trees. In other words, a die-off of this magnitude in the mixed conifer forest would completely offset 10 years of cumulated tree growth in terms of carbon storage. These results suggest that the forest sector sequesters less carbon than was previously estimated in standing dead trees and have implications for calculating the benefit of forest carbon offset projects.

## Project Benefits

Results from this project directly support the California Air Resources Board and its charge to implement AB 32 and are essential for resource managers and state policymakers. By improving the carbon stocks assessment consistent with international guidelines, the project supports efforts by the California Climate Action Registry to collect data on facility-level and entity-wide greenhouse gas emissions directed by the 2005 Integrated Energy Policy Report. Specifically, this research improves the accuracy and completeness of forest carbon accounting and greenhouse gas budgets for California mixed conifer forests. Adding critical detail on standing dead tree decay and demographic processes enables informed predictions of the capacity of California forests to sequester carbon. Implementing these improved estimates as a dynamic and repeatable forest sector greenhouse gas accounting provides a comprehensive and ecologically relevant approach for estimating rates of forest carbon emissions. For the first time, the project delivers original studies of standing dead tree carbon density and develops information specific to California mixed conifer forests and the full range of decay conditions quantifying resultant emissions. These initial greenhouse gas emission projections tied to catastrophic mortality events are a valuable first step toward anticipating the impact of widespread forest mortality on California forest ecosystems and on the region's greenhouse gas budget.

# **CHAPTER 1:**

## **Overview: Forest Carbon Inventorying and Monitoring**

### **1.1 Need for Forest Carbon Inventory and Monitoring**

As a direct result of well-documented increases in forest morbidity and mortality, standing dead trees (SDT) are becoming ever more important players in forest carbon dynamics. Tree death marks a critical transition in the carbon cycle when individual trees shift from growing carbon sinks to decaying carbon sources. These trees in transition play essential roles in the biogeochemistry and biodiversity of forests. Because of their ecological importance, SDT are also an essential component of greenhouse gas (GHG) inventory and monitoring. In continental US and Canada forests, SDTs form between 5% and 35% of aboveground forest biomass (Aakala et al. 2008, Vanderwel et al. 2008). In California mixed conifer forests, SDTs contain an average of 9.5 Mg carbon/ha, or 20.5 million metric tons of carbon (Battles et al. 2014). The forest carbon pools and fluxes to which SDTs contribute are the subject of inventory, regulation, and policy at state, federal, and international levels of government. In California, the Air Resources Board inventories and regulates GHG from forests and rangelands through the Global Warming Solutions Act, Assembly Bill 32. SDTs form one of five forest sector carbon pools included in the U.S. National Greenhouse Gas Inventory administered by the Environmental Protection Agency (EPA 2011) and built upon the US Forest Service's Forest Inventory and Analysis (FIA) monitoring program. In turn, the United Nations Framework Convention on Climate Change, a treaty agreement to stabilize GHG concentrations, relies on national GHG inventories (Woodall et al. 2013, GTR SRS 176, United Nations 1992). The Intergovernmental Panel on Climate Change (IPCC) also makes periodic assessments and methodology recommendations to countries and scientists conducting GHG inventories, using a similar set of categories with the addition of harvested wood. Because of the regulatory and policy implications of GHG inventories, accurate and ecologically relevant accounting is an essential component of global diplomacy.

### **1.2 IPCC Recommended Protocols**

The 2006 IPCC Guidelines for National Greenhouse Gas Inventories outlines a gain-loss approach to estimate GHG emissions (Aalde et al 2006, IPCC 2006). In this process-based approach, carbon stock changes within all subdivisions of a land use category (i.e., forests) are estimated by pool. The carbon pools assessed are above ground biomass, below ground biomass, deadwood (both standing and down), litter, soils, and harvested wood products. Accurate estimation of total GHG emissions relies on pool quantities, fluxes and movement between pools, and uncertainties. This approach to inventory is designed to include changes due to both discrete events such as insect outbreaks or timber harvests and continuous processes such as growth and decay. For consistent calculation and reporting, estimates of change in carbon stocks are reported in units of carbon, typically derived from units of biomass.

## 1.3 Past and Proposed Approaches to Forest GHG Accounting in California

The State of California enacted the Global Warming Solutions Act, or Assembly Bill 32, in 2006 (<http://www.arb.ca.gov/cc/ab32/ab32.htm>). The Act is intended to reduce potentially harmful changes in climate. It requires the Air Resources Board (ARB) regularly inventory GHG emissions, set statewide GHG emission limits, and develop regulations to reduce emissions. Within the GHG inventory, forest and rangeland ecosystems form one of the inventoried and regulated sectors.

Recent estimates for California's forest have varied greatly from a net carbon uptake of 15.7 million Mg y<sup>-1</sup> (Zheng et al. 2011) to net carbon loss of 0.4 million Mg y<sup>-1</sup> (USFS 2013). The most recent ARB GHG accounting effort for the sector, spanning 2000-2012, is based on a California Energy Commission study (ARB 2014). The study examines forests primarily in the northern half of the state from 1994 to 2000, predicting carbon gains and losses in other locations and in other years based on these patterns (Brown et al. 2004). The demands on GHG inventory have changed considerably since this report, as has data availability. A related study develops a revised method for inventory of GHG emissions from California forest and rangelands (Battles et al. 2014). The proposed stock change assessment approach encompasses all forest and rangeland areas within the state, focusing on 2001 through 2008. The methodology utilizes repeat measurements through time, continuous data generation, and moderate to fine resolution remotely sensed vegetation data. Minimum preliminary data processing is necessary, and estimates of uncertainty are attainable for all major components of the sector inventory. Additionally, the approach conforms to IPCC inventory guidelines (IPCC 2006, 2013b). The estimates indicate that the forest and rangeland sector was a net carbon source in 2001-2008, at an annual rate of 14 MMTC y<sup>-1</sup>. Declines in carbon density and reduction of analysis area were major drivers of the loss. These results provide the first spatial estimates of vegetation carbon changes and uncertainties for the entire state and establish the beginning of a time series to continuously monitor carbon emissions and sequestration in California ecosystems (Battles et al. 2014).

## 1.4 Gaps in Assessment of Standing Dead Tree Carbon

### 1.4.1 Biological Gaps

Standing dead trees are an important component of carbon dynamics in forested ecosystems, but are poorly represented in vegetation and earth systems models. During the standing dead transition state the carbon pool in trees changes in three important ways. Total volume of biomass is reduced (Aakala et al. 2008, Raphael and Morrison 1987), wood and bark density changes through decay and weathering processes (Krankina and Harmon 1995, Harmon et al. 2011, Domke et al. 2011), and tissue carbon and nitrogen content is also transformed through decay and weathering (Harmon et al. 2013). In the process, the demographic and decay processes of SDT shape forest habitat availability and carbon transfer rates and residence times, which are important biogeochemical indicators (Hilger et al. 2012). In fact, carbon residence time in forests, dependent on the dynamics of SDT, is the largest source of uncertainty in the global vegetation models that predict response to global change (Friend et al. 2014). This

transitional period between growth and decomposition on the forest floor needs to be quantitatively described in order to understand the role of SDT in forest carbon pools and fluxes, to provide realistic estimates of broader ecosystem processes, and to accurately project ecosystem greenhouse gas budgets.

#### 1.4.2 California Challenge

In the recent past, SDT formed about 11% of standing trees and 7% of total standing carbon in California mixed conifer forests (FIADB 2011, Woodall 2012). Within the past decade, however, California forests have experienced dramatic increases in mortality. Tree mortality in California is most often attributable to disturbances and environmental conditions including insect outbreaks, episodic disease, climate, chronic air pollution, and fire. Many of these factors have intensified and compounded, resulting in a higher proportion of SDT relative to live trees. For example, the number of standing dead sugar pine trees in Sequoia-Kings Canyon National Parks (29% of live stems) is four times greater than average for this species in California (7% of live stems, FIADB 2011). The cause of the increased mortality is thought to be the combined effects of white pine blister rust, an exotic fungal pathogen, and exposure to high levels of ozone and nitrogen pollution (Battles et al. 2013). In Sierra Nevada old growth forests, tree mortality rates across all species have more than doubled in recent decades (van Mantgem and Stephenson 2007). In 2008-2009, irruptions of bark beetles in California's coniferous forests caused a 200-300% increase in pine tree deaths at sites throughout the state. During the same period, white fir mortality in some locations increased 1000% due to outbreaks of fir engraver beetle (FIADB 2011). These episodes parallel the unprecedented outbreaks of bark beetles throughout comparable forests in the western United States and Canada, which have decimated millions of hectares of forest. Climate change projections and air pollution trends indicate a future of exacerbated environmental stress both for California's forests (Battles et al. 2009; Moser et al. 2009) and forests throughout the western United States (Allen et al. 2010 ). Elevated tree mortality will drive local increases in GHG emissions and is likely to transform impacted forest ecosystems from effective sinks to sources of atmospheric C and N greenhouse gas compounds. However, the demographic attributes of SDT in California forests, including their decomposition trajectories and standing dead longevity, remain unknown. To improve the accuracy and ecological relevance of GHG inventory for California's forest and rangeland sector, a better understanding of the decay patterns and fall rates of SDT in our forests is needed.

**Figure 1: Current standing dead and dying trees, Sequoia National Park**

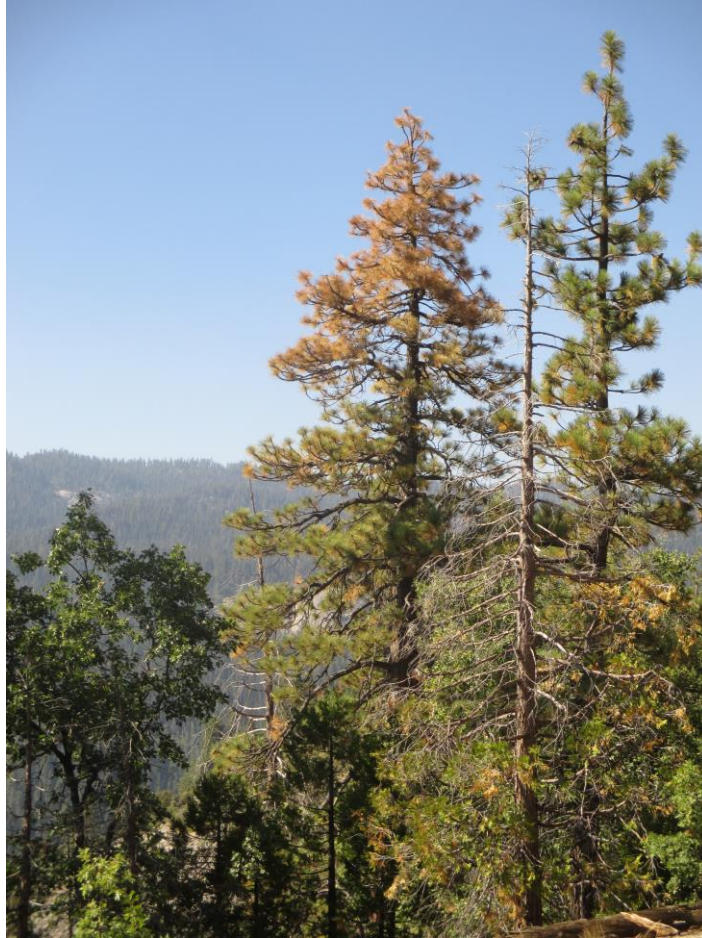


Photo credit: S. Cousins

### 1.4.3 National Challenge

Forest inventories and carbon accounting efforts in particular have traditionally focused primarily on growing stock and secondarily on fuels. In these cases, dynamics of SDT are often roughly estimated or even omitted. Currently, nationwide ground-based inventory of forest carbon relies on the US Forest Service's FIA framework. As of the year 2000, the FIA program has coupled a nationwide approach to inventory with an extensive network of forest plots, making periodic continental-scale assessments of standing biomass feasible (Heath et al. 2009). The FIA approach to biomass calculations, known as the Component Ratio Method, sums the carbon-containing components of each tree. Volume of each component is calculated according to equations developed for each tree species within each region, with live and dead standing biomass treated in the same manner (Woodall et al. 2010, Woudenberg et al. 2010). Total bole biomass relies on a visual approximation of the cull (rotten or unmerchantable) timber volume. This a major obstacle in accurate estimation of SD biomass, because it fails adjust for the *in situ* structural and density losses that characterize SD trees (Heath et al. 2011, Smith et al. 2003). Additionally, information on the duration any given SDT will remain standing is scarce. The fall rates of SDT vary with species, region, and many site factors, and are important in shaping the path and rate of wood decomposition, thus influencing forest emissions (Hilger et al. 2012).

A variety of empirically-based decay adjustment factors are in development. These are designed to lend greater accuracy and relevancy to forest carbon accounting efforts, and focus on both standing dead and down woody debris (Harmon et al. 2011, Domke et al. 2011). However, none of the recommended methods have thus far been implemented in regional or national carbon or GHG estimates. An integrated model that combines the effects of these diverse decay processes from a carbon dynamics standpoint is needed to estimate net effects on carbon and GHG budgets.

## **1.5 Overview of this Project**

### **1.5.1 Measure the Carbon Density in Standing Dead Trees in California Mixed Conifer Forests**

In this study, the authors describe the roles of SDT in forest carbon dynamics using three approaches. First is an assessment of changing carbon density within individual trees (Chapter 2). This investigates the patterns of density and carbon loss within standing dead trees as they decay. Empirical measurements take a dimensional analysis approach, sampling wood and bark properties from trees in the decay classes used nationwide by the FIA program. Next, the degree to which tissue density and carbon concentration varies with tree species, decay class, and tissue type is determined. These decay patterns are then used to develop density reduction factors and net carbon reduction factors for each of the major species in California mixed conifer forests. The resultant SDT biomass and C stock estimates are applied in refining the estimates of carbon stored in SDT in California's most common forest type, mixed conifer.

### **1.5.2 Quantify the Fall Rates of Standing Dead Trees in the California Mixed Conifer Forests**

Next, the authors examine longevity of SDT on the landscape (Chapter 3). Two long-term studies of SDT are used to determine the fall rates of SDT in California mixed conifer forests and the major drivers of these patterns. For both sites (Blodgett Forest Research Station and Southern Sierra National Parks), the shape and magnitude of fall rate curves are determined first, then variations attributable to species identity and tree diameter are quantified. The tree fall rates and patterns presently observed are then further compared to previous and historic studies of SDT in California mixed conifer forests. The longevity of SDT yields a description of the residence time of upright dead biomass in forests and thus sheds light on the degree and duration of the decaying carbon pool.

### **1.5.3 Enhance Current Methods to Assess Gain-Loss of Carbon from Standing Dead Trees in California's Conifer Forests**

The final synthesis uses the measured carbon density and demographic rates to estimate the contribution of standing dead trees to carbon gains and losses in California mixed conifer forests (Chapter 4). This stage of the study combines the biomass losses seen in the dimensional analysis with landscape scale inventory from the FIA program forest plots in California mixed conifer forests. Using the empirically-based density reduction factors and fall rates ultimately makes it possible to generate an accurate estimate of losses of carbon from SDT.

This chapter also assesses the feasibility of continuous statewide GHG accounting of dead trees, evaluating the FIA program products, LANDFIRE, and related land data tools.

# CHAPTER 2: Carbon Density of Standing Dead Trees in California Conifer Forests

## 2.1 Introduction

### 2.1.1 Background

Standing dead trees (SDTs) are essential structural, biological, and biogeochemical components of functioning forest ecosystems. Importantly, they host the first stages of decomposition and nutrient recycling, releasing stored carbon back to the atmosphere and forest floor (Whittaker et al. 1979, Spears et al. 2003). These first phases of decay set the stage for the ongoing weathering and breakdown of organic matter that proceeds for many years following. SDT are also irreplaceable habitat centers for many species, serving as locations for nesting, denning, and foraging, and as high visibility sites for hawking or display (Thomas 1979, Kruys et al. 1999, Bunnell and Houde 2010). In forests nationwide, SDT form a small but growing carbon pool, typically  $<1\text{MgC ha}^{-1}$  (Woodall et al. 2012). In California forests, SDT represent a much larger proportion of the forest carbon pool (Battles et al. 2014). On average, SDTs in California forests contain  $3.5\text{ MgC ha}^{-1}$  representing 6% of total live tree carbon. In conifer dominated forests, SDT carbon is even higher. For example, in California's vast mesic mixed conifer forest, SDTs have an average carbon density of  $9.5\text{ MgC ha}^{-1}$  and store 20.5 MMTC (million metric tons of carbon, Battles et al. 2014).

In California mixed conifer forests, mortality rates have recently climbed to unprecedented levels. While SDT once formed an average of 11% of stems and 7% of total standing carbon, SDT abundance has doubled and tripled in many mixed conifer forests (FIADB 2011, Woodall 2012). Drought, irruptions of bark beetles, disease, pollution, and land management legacies have all contributed to this trend (van Mantgem and Stephenson 2007, Allen et al. 2010, FIADB 2011, Battles et al. 2013). Many of these forest stressors act in combination with each other and are increasingly exacerbated by the effects of global change. Regionally increased mortality rates only foreshadow the forest degradation expected throughout the North American West as warmer, drier climates drive additional mortality (IPCC 2007, van Mantgem et al. 2009). In a related ARB study, Battles and others documented declines in the carbon density of California forests and in forest and rangeland area during 2001-2008 (Battles et al. 2014). These shifts fueled a net carbon loss of  $14\text{ MMTC y}^{-1}$  from the forest and rangeland sector during that period. While many factors drive this carbon loss, tree death, particularly in areas of catastrophic (>90%) mortality, contributes substantially to both declines in total aboveground carbon density and to conversion of vegetation types.

As trees stand dead in the forest, their biomass and carbon pools transition away from the live state. Total volume declines through loss of leaves, twigs, and branches, losses obvious to the casual observer (Aakala et al. 2008, Raphael and Morrison 1987). More subtle are the wood density and bark density declines due to fungal decomposition and excavation by xylophagous (wood eating) insects (Krankina and Harmon 1995, Harmon et al. 2011, Domke et al. 2011).

Tissue chemistry, particularly carbon and nitrogen content, is often modified in the process of decomposition (Harmon et al. 2013). The effect of biomass loss from individual SDTs on the forest carbon cycle is that trees become net emitters of carbon, thus counteracting the forest's widely documented carbon gains. Elevated tree mortality will drive local increases in GHG emissions and is likely to transform impacted forest ecosystems from effective sinks to sources of atmospheric carbon and nitrogen greenhouse gas compounds. However, the quantity and trajectory of decay-driven biomass losses that SDT in California forests follow remains unknown. As California forests are pushed toward increased mortality and greater SDT abundance, it is critical to understand the patterns of SDT decay that shape carbon dynamics and the resulting forest GHG budgets.

### 2.1.2 Problem Statement: Current Approaches for Biomass Estimates in SDT

Current approaches to forest inventory and carbon accounting fail to adjust for the structural and density losses that characterize SDT (Heath et al. 2011, Smith et al. 2003). As described in Chapter 1, treatments of SDT in FIA-based inventories assume that all standing trees have wood with live tree properties. However, it is clear that through weathering and decay, the chemical and physical attributes of tree tissues can change substantially during the time an SDT remains standing.

In order to provide a functionally relevant account of SD biomass, a number of modifications to the FIA framework have recently been proposed. Research on the trend of biomass loss in standing dead trees has led to the development of Structural Loss Adjustments (SLA) for species in the Great Lakes region (Domke et al. 2011). To better describe the changing density throughout the wood and bark that remains in place, Harmon (2011) and others have developed suites of Density Reduction Factors (DRF). The DRF are developed by extensive measurement of specimens, then applied by decay class to standing and down dead wood. Harmon (2013) has also examined the changing composition of SD and down dead tissues. They have found that C concentration generally rises with advancing decay, though this effect is modified by live wood chemistry and thus varies among species. Most accounting efforts treat carbon biomass as 50% of total biomass, but Harmon and colleagues' (2013) work suggests that this underestimates C concentration by 5-10%.

However, the recommended methods to improve deadwood biomass estimates (DRF, C concentration adjustment, and SLAs), have thus far been implemented only in experimental regional inventories, and then only in separate applications (Domke et al 2011, Harmon et al. 2011, Harmon et al. 2013). For California forests, an integrated model that combines the effects of these diverse decay processes from a broader C dynamics standpoint is needed to meaningfully estimate net ecosystem effects on C and GHG budgets.

### 2.1.3 Carbon Density Study Objectives

This study utilizes a dimensional analysis approach to estimate in situ decomposition of standing dead trees in the mixed conifer forests of California. The approach is explicitly designed to take advantage of the decay classification used in the Forest Inventory and Analysis (FIA) program for standing dead trees (Thomas 1979, USDA Forest Service 2010). The degree to which tissue density and C concentration varies with tree species, decay class, tissue type, and

relative position is also determined. These decay patterns are then used to develop density reduction factors and biomass transfer equations for the dominant tree species in each decay class. The resultant SDT biomass and C stock estimates can be applied in refining the estimates for carbon stored in SDT in California's most common forest type.

## 2.2 Methods

### 2.2.1 Site Descriptions

Blodgett Forest Research Station (BFRS) is situated on the western slope of the Sierra Nevada near Georgetown, California (38°52' N; 120°40' W). Forest composition is predominantly mixed coniferous. Six native tree species are commonly found in mixtures of varying proportions: white fir (*Abies concolor*), incense cedar (*Calocedrus decurrens*), coast Douglas-fir (*Pseudotsuga menziesii* var. *menziesii*), sugar pine (*Pinus lambertiana*), ponderosa pine (*Pinus ponderosa*), and California black oak (*Quercus kelloggii*). The elevation of study sites ranges from 1220 to 1350 meters. Annual precipitation at BFRS averages 1660 mm, with a Mediterranean climate pattern of warm summers (14-17°C) and mild winters (0-9°C). Soils are derived from granodiorite parent material and are considered productive for the region. The study areas at BFRS were heavily cut in the early twentieth century and later regenerated naturally, a land use pattern common throughout the mixed conifer forest elsewhere in the Sierra Nevada range. A detailed description of BFRS management, growth, yield, and trends is found in Olson and Helms (1996). Carbon density studies on SD trees at BFRS were carried out in both reserve stands and those actively managed for timber production.

The southern Sierra study sites are co-located with the US Geological Survey Western Ecological Research Station (USGS-WERC) Forest Demography Study. This long term study of forest plots in Sequoia, Kings Canyon and Yosemite National Parks provides crucial estimates of key drivers of forest change, namely tree growth, survival, and recruitment. The five plots with carbon density sampling are montane mixed coniferous, dominated by red fir (*Abies magnifica*) and white fir, with giant sequoia (*Sequoiadendron giganteum*), incense cedar, and sugar pine also present in significant numbers. All are located in the Giant Forest and Panther Gap areas of Sequoia National Park (36°34'N 118°44'W). At elevations of 2000-2600 meters, precipitation for these sites averages 1200mm/yr with 35-65% in the form of snow. Soils are coarse loams from granitic parent material. The study locations have not been logged, have not experienced fire within the past ten years, and have been without a stand-replacing disturbance for several centuries (Caprio and Swetnam 1993, Das et al. 2007). USGS-WERC scientific staff have conducted an annual census of all trees above 1.37 meters since establishment of these plots (1982-1992). As part of this effort, trees that have died within the past year are evaluated for factors contributing to mortality (van Mantgem and Stephenson 2007). Structural and habitat characteristics of standing dead trees, including FIA decay class, are described during this survey. Sampled trees from the USGS-WERC sites are trees that fell by natural processes in 2012-2013. Because of the annual inventory, each study tree has a known year of mortality and tree fall.

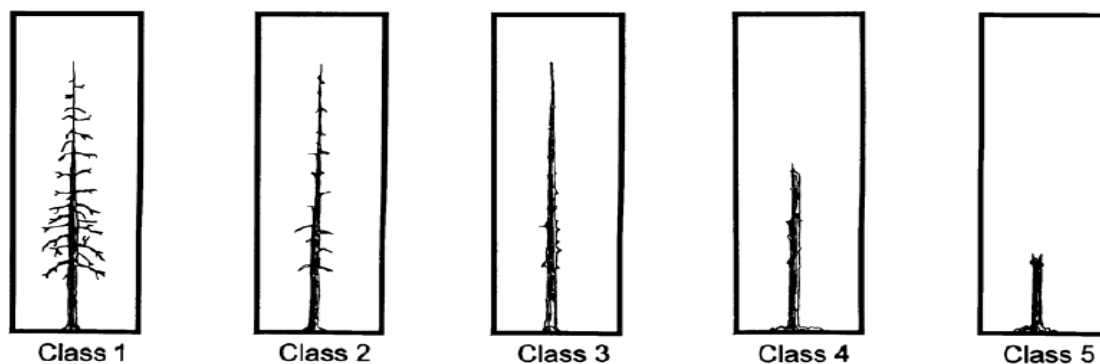
## 2.2.2 Sampling Regime

### 2.2.2.1 Selection and Standing Dimensions

Standing dead trees were identified at BFRS and in the USGS-WERC study areas through use of previous inventories and the observations of site managers. From these candidate SD trees, trees were selected for the study to maximize sampling across FIA decay classes 1-5, to include individuals across a range of diameters above 20cm at breast height, and to represent all major species present in the mixed conifer forest. Specifically excluded were trees where fires were a contributing factor in mortality, and also excluded trees with severe mechanical wounds from logging operations. Study trees at BFRS were standing during selection and field data collection, then felled for further measurement and sampling. Study trees in USGS-WERC areas were the product of natural treefall and were measured while prone.

Each SD tree in the study was classified according to the USFS FIA program's decay class system (Figure 2). This classification is based upon the structure and condition of the tree's top, branches and twigs, bark, sapwood, and heartwood, and is used for SD trees throughout the FIA's nationwide forest inventory plots. (USFS 2010, after Thomas 1979). In addition to decay classification, upright measurements included diameter at breast height, percent bark present, height, proximal cause of death, limb and twig condition, wood hardness, use by woodpeckers, and cavity count. This data was collected according to the Blodgett Forest Inventory Protocol (Blodgett Forest 2008). Because broken and decaying treetops take on many forms, broken boles were further classified using four standard shapes: intact, flat (a horizontal break), tapered (remnant portion of bole tapers to a point), and stairstep (remnant portion of bole tapers naturally and upper break is flat). This classification permits later estimation of the wood and bark volume represented in the odd wood volumes resulting from breakage, and the development of accurate structural loss adjustments for mixed conifer species. The dimensions of SD treetops were obtained using a sonic Vertex hypsometer (Haglöf Inc., Madison, MS) and a Criterion 400 Laser (Laser Technology, Inc. Centennial, CO). For trees with broken boles, the remnant portion was estimated as a percentage (nearest 10%) of original volume; dimensions of broken portions were measured to the nearest 0.5 meter. Following upright measurements, the selected SD trees were carefully felled by a professional sawyer. Felling SD trees can be extremely hazardous, so the sawyer was able to exclude any tree deemed unsafe. After felling, each tree's location and felled condition was noted.

**Figure 2: Forest Inventory and Analysis Decay Class Framework**



Decay class	Limbs and branches	Top	% Bark Remaining	Sapwood presence and condition	Heartwood condition*
1	All present	Intact/ pointed	100	Intact; sound, incipient decay, hard, original color	Sound, hard, original color
2	Few limbs, no fine branches	May be broken	Variable	Sloughing; advanced decay, fibrous, firm to soft, light brown	Sound at base, incipient decay in outer edge of upper bole, hard, light to reddish brown
3	Limb stubs only	Broken	Variable	Sloughing; fibrous, soft, light to reddish brown	Incipient decay at base, advanced decay throughout upper bole, fibrous, hard to firm, reddish brown
4	Few or no stubs	Broken	Variable	Sloughing; cubical, soft, reddish to dark brown	Advanced decay at base, sloughing from upper bole, fibrous to cubical, soft, dark reddish brown
5	None	Broken	Less than 20	Gone	Sloughing, cubical, soft, dark brown, OR fibrous, very soft, dark reddish brown, encased in hardened shell

\* Characteristics are for Douglas-fir. Dead trees of other species may vary somewhat. Use this only as a guide.

Source: USDA Forest Service 2010

### 2.2.2.2 Dimensional Analysis

Standing dead trees are often host to a wide range of wood conditions, ranging from sound to extensive decay. The measurements and tissue sampling of felled SD trees were designed to capture the patterns and variation in this heterogeneity from tree base to top and exterior to interior. The measurement and sampling protocol builds upon dimensional analysis techniques and earlier work with both standing dead and down dead wood inventories (Harmon et al. 2011, Whittaker and Woodwell 1968). Felled trees were first marked into 1-3 sections dependent on size: for logs 0-2m, 1 section; 2-10m, 2 sections; and over 10m, 3 sections. Entire SD volume was measured by length and the diameters at each section boundary. All diameters were noted as bark on or bark off. The base section was 2m in length and upper sections divided the

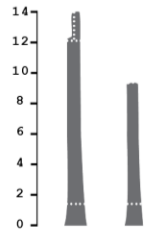
remaining length equally; this arrangement was designed to describe wood condition at the forest floor and as affected by root pathogenic fungi as compared to that at canopy level. Then, the dimensions and attributes of each section diameter, length, bark thickness, bark presence (nearest 5%), wood hardness (1-5 scale) were measured. The length to highest intact diameter and form of the bole above this point was recorded for purposes of describing wood volume.

Following bole volume measures the felled trees were dissected to assess longitudinal and radial variation in tissues (Figure 3). The same tree sections were used, with wood and bark samples taken from the midpoint of each section whenever feasible. First, using hand tools or a chainsaw (Stihl Model MS362), a 5-15 cm cross sectional sample, or "cookie" was cut from the midpoint of each log section. This cut also provided a clean cross-sectional face to examine radial decay. The wood condition of the face was described by means of three pith-to-bark radial transects, the first random and others at 120° and -120° from the first. Each transect was segmented and measured according to the wood type at the surface. Structurally sound wood with limited galleries and decay present was classified "hard". Wood delaminated along one or more axes, unable to hold its form under pressure, or with many galleries and extensive decay was classified "soft". Internal cavities, excavations, or galleries greater than 0.5 cm on the transect were classified "gone" (density=0). Wood type determinations were made by using a chaining pin, axe, or small knife to penetrate and dissect adjacent tissue. As a check of the radial transects, a visually estimate of the total cross sectional area in each wood type (nearest 5%) was also recorded.

Samples of bark and of each wood type present in each section were obtained in order to measure SD tree tissue density and carbon content. Hard wood samples were collected as whole or partial cookies. Bark samples averaged 130 cm<sup>3</sup>. For soft wood, the green volume was measured in the field to the nearest millimeter using a ruler or calipers (average sample volume = 640 cm<sup>3</sup>). Sample cutting and trimming with a knife or fine saw was conducted on a clean, flat surface to avoid mixing the soft tissues among trees or sections. For extremely soft wood, a measured area was marked on an intact surface then excavated into a sample bag (Figure 3). Finally, all friable samples were transferred to labeled bags for transport to the lab.

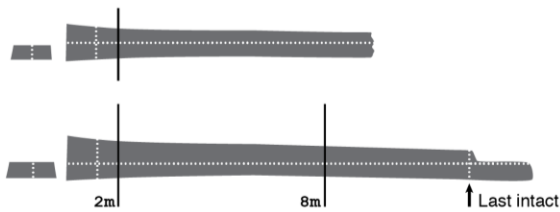
**Figure 3: Technique for Dimensional Analysis; Sampling and Measuring Volume of Decayed Wood**

**A. Standing**



1. Decay classification
2. Standing dimensions
  - DBH
  - Height
  - Top form
3. Habitat features
4. Other characteristics

**B. Down - Whole**



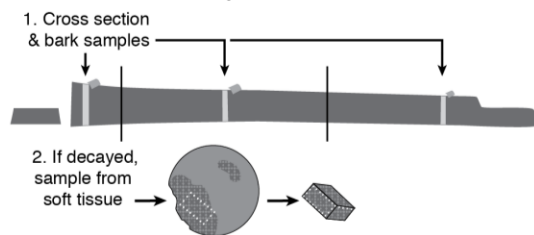
1. Down bole dimensions
  - DBH
  - Full length
  - Last intact length and diameter
2. Identify sections
  - <10m = 2 sections; >10m = 3 sections

**C. Down - Sections**



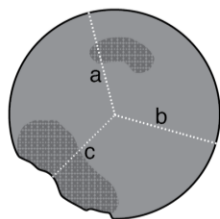
1. For each section end:
  - Measure bole diameter
  - Record bark thickness
2. For each entire section:
  - Record bark percentage
  - Classify wood hardness

**D. Section Samples**



1. Sample from section midpoint if present:
  - Intact/hard wood cross sections
  - Bark
2. If decay is evident:
  - Sample decayed tissue, keep density unchanged
  - Measure green volume of sample

**E. Radial Transects**



1. Three radial transects at each section midpoint:
  - First random, then 120° apart
  - From center outward, test condition w/ pin or knife
  - Record distances intact, decayed, and absent

Art credit: S. Cousins

### 2.2.2.3 Wood Volume and Density Determinations

Tissue samples arrived from the field as pre-cut soft wood samples, hard wood cross sections (full or partial), and bark from each section. Prior to drying, green volume was measured. Hard wood samples were cut into radial blocks using a 12-inch miter saw (Hitachi C12FDH) and custom jig, and then measured with a ruler or calipers. Green volume of hard blocks averaged 170 cm<sup>3</sup>. Due to its irregular shape and absorbent properties, the volume of bark samples was determined using displacement in water. First, bark samples were fully saturated by repeated submersion and tracking the volume of water displaced at each iteration. Then, the total volume of displaced water was determined using a displacement vessel (volumetric edema gauge (Baseline Evaluation Instruments, White Plains, NY)) or overflow canister (Scientific Equipment of Houston)). The displaced water was collected and weighed to the nearest 0.1 mL on a balance (Model P1200-00V1, Sartorius AG, Goettingen, Germany) to determine mass and thus the volume of the bark sample. All wood and bark samples were then transferred to Kraft paper bags and placed in a drying oven at 100-105°C; a small number of bark samples were dried at 80°C. After 48 hours, the samples were weighed at intervals of 24-96 hours and removed when they reached a constant dry weight (Bergman 2010). Wood and bark density was calculated as the ratio of oven dry mass (g) to green volume (cm<sup>3</sup>) at room temperature. This value can also be interpreted as the basic specific gravity (Williamson and Wiemann 2010).

The majority of dried samples, representing trees from all species and decay classes, were then finely ground for chemical content analysis. Samples were ground using a #4 Wiley mill fitted with a 0.5 mm screen. If needed, fibrous remains were ground in a small coffee mill. The resultant powder was thoroughly mixed, and a minimum of 3g retained for analysis. The University of California Davis Analytical Laboratory (UCDAL) performed analysis of total carbon and nitrogen presence by weight. The analytical method used was sample combustion in a muffle furnace, which converts organic and inorganic substances into gases. The gases are detected and measured by thermal conductivity/IR detection using a TruSpec CN Analyzer (Leco Corporation, St. Joseph, MI)(Association of Analytical Communities 2006).

### 2.2.3 Allometric Scaling

Standing dead tree carbon density and density reduction factors are dependent upon both the quantity (volume) and quality (density and chemical composition) of wood and bark in SD trees. Both are subject to processes of weathering and decay, which is known to affect a tree's many tissues and structural components in different ways. Therefore, density and carbon content of individual trees were calculated specific to tree section and tissue type. First, total bark-off tree volume was calculated using measured diameter and height in combination with taper equations specific to mixed conifer species observed in the Sierra Nevada (Biging 1984). When total tree height was unavailable (i.e., the bole was broken), SD tree heights were regressed from diameter using the model  $\ln(Ht) = B_0 + B_1 \cdot \ln(DBH) + B_2 \cdot \ln(DBH) \cdot \ln(DBH)$  with coefficients specific to BFRS (Holmen, unpublished data, 1990). The resulting total SD volume was allocated to each section and wood type based on the section measurements and radial transects described above. The surface area per type at the midpoint cross section was calculated to determine the volume of each wood type specific to section. To do so, distance along the transect (nearest 0.5cm) was treated as a partial (1/3) annulus, and the proportion of

each tissue (wood hard, soft, or gone) was formed by the weight of annulus areas. The mean of the three sectors on each radial transect formed the section's surface area. Next, a weight (0.0 – 1.0) was assigned to each wood type within each tree section. Bark volume was later added to each section in proportion to volume, measured midpoint bark thickness (nearest 0.1mm), and bark presence while standing (nearest 5%).

#### 2.2.4 Whole Tree Biomass, Density Reduction Factors and Carbon Density

Tissue density and composition were tied directly to measured volumes in individual trees and their spatially explicit biomass components. In determining whole tree biomass and carbon content, weights for each wood type (hard, soft, or gone) by section were first used to reconstruct volume present by type. Biomass per tissue type (kg) is the product of volume and density, with measurements specific to the samples from that section. Carbon content was then calculated as the product of tissue type biomass and carbon concentration by weight, which was also analyzed specific to sample and section. Finally, whole tree biomass and carbon content are the sum of the component sections. Whole tree density and carbon concentrations are calculated from the total SD volume and total biomass and carbon content, respectively. A density reduction factor (DRF) was then computed for each SD tree. DRF is the ratio of dead density to live density for a tree of equal volume (Harmon et al. 2011). Density reduction factors reported by tree species and decay class are the mean of individual trees within each group.

#### 2.2.5 Analysis

Because users of density and carbon content measurements may aggregate this data in a number of ways, the SD tree analysis was compiled using a variety of common aggregation levels and dependent variables. Response variables include wood and bark density, wood and bark carbon concentration by weight, total wood biomass, and total wood carbon. These were examined in groups according to FIA decay class, tissue (wood and bark), position, and taxon.

### 2.3 Results

#### 2.3.1 Volume and Wood Density Loss

The SDT sampled in the study represent all six major mixed conifer species in each of five FIA decay classes across broad range of sizes (Table 1). Notably, of 109 total SDT measured and sampled, 31 are assigned to decay class 4 and 17 to decay class 5. These are the most advanced decay conditions, and therefore the rarest and least studied SD trees. The sampled standing dead trees represent the bulk of standing dead biomass in mixed conifer forests: all are over 12.5cm (5 inches) DBH and 95% measure between 20cm and 100cm DBH.

As anticipated, wood density of SDT declined with decay class (Table 2). Live wood density for the six mixed conifer species ranges from .34 (incense cedar) to .45 (Douglas fir) g/cm<sup>3</sup> (Forest Products Laboratory 2010). From all trees sampled, mean live density was 0.376 g/cm<sup>3</sup>.

**Table 1: Standing Dead Tree Characteristics by Species, Decay Class, and Diameter Class**

Species	Decay class (n)					Diameter class (cm DBH)			Total SD Trees
	1	2	3	4	5	12.5-30	30-50	>50	
White fir	5	6	4	10	4	10	10	9	29
Red fir	6	3	0	1	0	4	3	3	10
Incense cedar	0	4	6	3	3	10	5	1	16
Sugar pine	6	1	4	2	2	3	6	6	15
Ponderosa pine	3	1	6	8	5	5	14	4	23
Douglas-fir	4	0	2	7	3	4	6	6	16
All species	24	15	22	31	17	36	44	29	109

Standing dead trees in decay class 1 were only slightly lower density, averaging 0.36 g/cm<sup>3</sup>. Each class progressively decreased, with decay class 5 averaging .21 g/cm<sup>3</sup>. Across all species, DRFs followed the same pattern, declining from near-live density (DRF=0.95; class 1) to close to half of live wood density (DRF=0.55; class 5). Among decay classes, class 3 showed the highest standard error in both density and resulting DRF (DRF SE=0.06), followed by classes 5 and 4 (DRF SE=0.05 and 0.04).

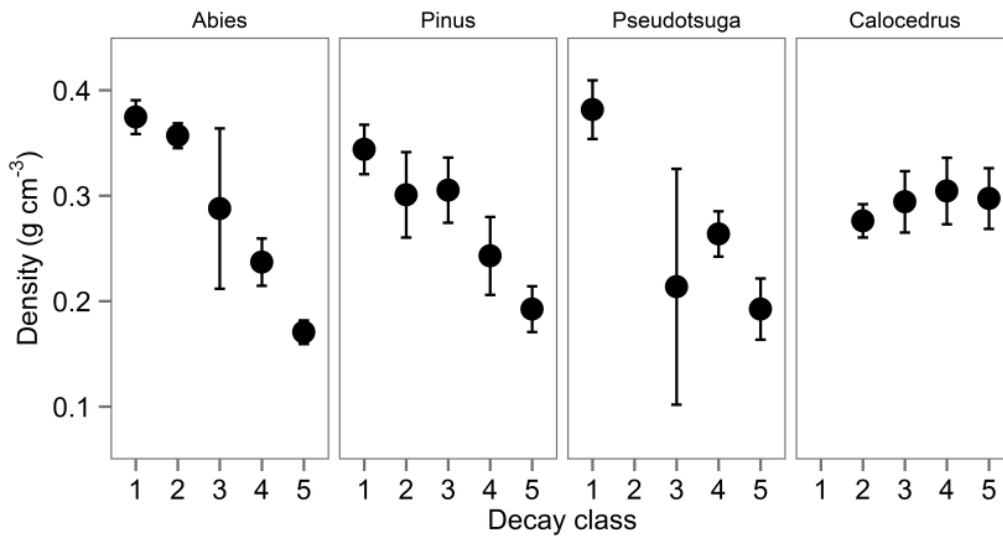
The pattern of density decrease was most evident in white fir, Douglas fir, ponderosa pine, and sugar pine (Table 3, Table 4). Each of these species demonstrated a marked decline from decay classes 1-3 to classes 4-5. White fir and Douglas fir had greater density losses at decay class 5 (DRF= 0.43 ± 0.05 and DRF=0.37± 0.03) than did either of the pines. Incense cedar did not show declines in density: wood samples from decay classes 4-5 were in fact more dense than live wood on average. Red fir had too few samples in advanced decay (n=1) to determine a trend.

**Table 2: Mean Combined Standing Dead wood and Bark Density and Dead:Live Density Ratio for Each Decay Class**

Decay class	SD density (g/cm <sup>3</sup> )	SE	Dead:live* density ratio	SE	n
1	0.36	0.01	0.95	0.03	24
2	0.33	0.01	0.88	0.02	15
3	0.29	0.02	0.81	0.06	22
4	0.25	0.02	0.65	0.04	30
5	0.21	0.02	0.55	0.05	16

\*Live density, Miles and Smith 2009. All other data this study

**Figure 4. Density (g cm<sup>-3</sup>) of Decay Classes 1-5 by Tree Taxonomic Group**



### 2.3.2 Carbon Concentration and Total Carbon Biomass as a Function of Species and Decay Class

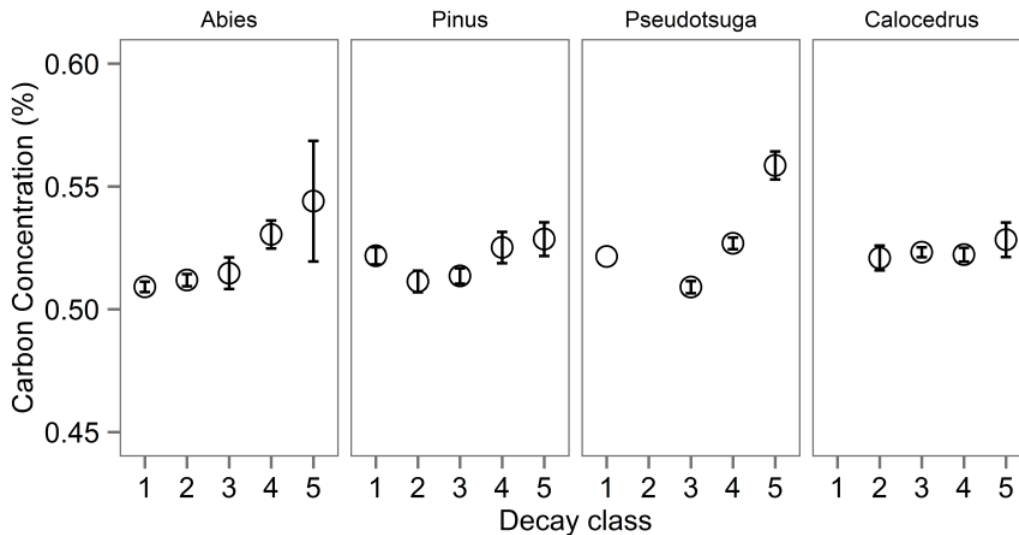
Wood and bark from all sections of 76 SDT representing six species and five decay classes were sampled for carbon and nitrogen concentration of tissues by weight. Across all sampled SDT, C concentration of combined wood and bark tissues climbed two to three percent by the final decay class (Table 3). White fir and Douglas fir demonstrated the largest changes. Ponderosa and sugar pine also showed increased C concentration, with slightly greater variation between decay classes (Table 6). Standing dead incense cedar maintained a constant carbon concentration of 0.52 in all decay classes. As with density, the change from live wood conditions was characterized by calculating the ratio of live C concentration to that of SD, forming a C concentration adjustment factor. When compared to an assumed live C concentration of 0.50, early-stage decay SDT (classes 1-3) were uniformly higher in C than live trees (adjustment factor > 1.00). Standing dead trees in advanced stages of decay (classes 4-5) were higher still, with adjustment factors ranging from 1.03 to 1.06.

**Table 3: Mean Combined Standing Dead Wood and Bark Carbon Concentration and Dead:Live Carbon Concentration Ratio for Each Decay Class**

Decay class	SD Carbon conc. (%)	SE	Dead:live* C conc. ratio	SE	n
1	51.37	0.24	1.03	0.00	11
2	51.45	0.23	1.03	0.00	10
3	51.51	0.21	1.03	0.00	14
4	52.72	0.28	1.05	0.01	27
5	53.71	0.54	1.07	0.01	14

\*Live carbon concentration 50%

**Figure 5: Carbon Concentration of Decay Classes 1-5 by Tree Taxonomic Group**



### 2.3.3 Bark Decay Patterns and Effect on Whole Tree Biomass

Behavior of bark during the SD decay process was distinct among species. The importance of bark to total SDT volume changed with decay class: in white fir, Douglas fir, and incense cedar, relative bark volume increased; the pines and red fir showed no trend (Table 7). Bark presence declined through decay classes, but density of extant bark was no less than 87% that of live trees. Inclusion of bark increased the whole tree density and total biomass in decay classes 3, 4, and 5 for all species except incense cedar (Table 7, Table 8).

**Table 4: Wood Characteristics: Mean Standing Dead: Live Density Ratio and Mean Carbon Concentration for Each Decay Class**

Decay class	DRF (Dead:live* density)	SE	n	Carbon concentration	SE	n
1	0.90	0.04	24	0.51	0.00	11
2	0.84	0.03	15	0.51	0.00	10
3	0.81	0.06	22	0.51	0.00	14
4	0.62	0.05	30	0.52	0.00	27
5	0.53	0.05	16	0.53	0.01	14

\*Live wood density, Miles and Smith 2009; all other data this study.  
Species listed separately in Table 7

**Table 5: Bark Characteristics: Mean Standing Dead:Live Density Ratio and Mean Carbon Concentration for Each Decay Class**

DRF (Dead:live* density)	SE	n	Carbon concentration	SE	Number of trees
1.17	0.06	24	0.53	0.00	11
1.01	0.04	15	0.53	0.00	10
0.96	0.06	21	0.53	0.00	13
0.92	0.04	27	0.55	0.00	25
0.87	0.08	10	0.57	0.01	9

\* Live bark density, Miles and Smith 2009; all other data this study.  
Species listed separately in Table 8

#### 2.3.4 Net Change in Biomass and Carbon Stored

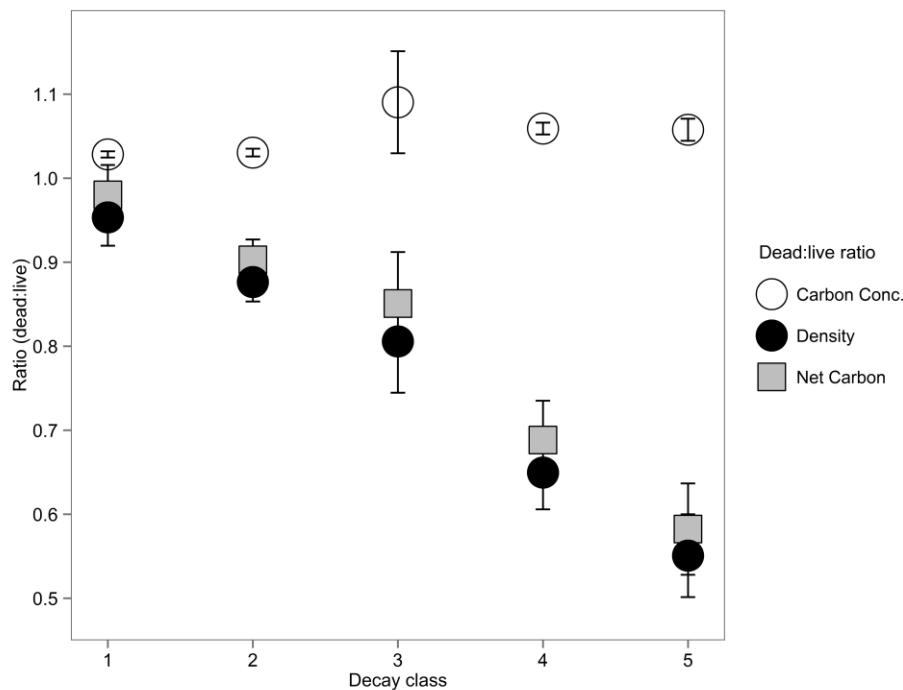
Decay in SDT is a combined pattern of substantial density loss and a subtly increasing C concentration. The net result is an overall loss of C as decay advances. Relative to live trees, C content (mean kg/tree) declines even in the first decay class (Table 3). For all species, SDT in classes 1 and 2 contained 92% of live tree carbon. Through the course of decay this dropped to 64% (class 4) and eventually 51% (class 5) of live tree carbon. Thus, although the chemical composition of wood and bark is altered by decomposition, the physical pattern of declining wood density drives loss of nearly 50% of carbon biomass in the most decayed SDT.

**Table 6: After Density Losses and Carbon Gains, Mean Dead:Live Net Carbon Ratio of Combined Wood and Bark for Each Decay Class**

Decay class	Dead:live* net C ratio	SE	Number of trees
1	0.94	0.04	11
2	0.89	0.03	10
3	0.85	0.07	14
4	0.68	0.05	27
5	0.60	0.06	14

\*Live carbon concentration 50%

**Figure 6: Standing Dead Tree Carbon Concentration, Density (DRF), and Net Carbon Density Relative to Live Trees for Each Decay Class**



Ratios are mean standing dead value: mean live value (Miles and Smith 2009). Density values are from measured SDT (n=107); carbon concentration and net carbon density values from SDT (n=76) resampled by Monte Carlo simulation. Error bars are standard error for all measurements.

## 2.4 Discussion

### 2.4.1 Patterns in Biomass Loss

The trend of biomass loss measured in SDT from California mixed conifer forests is consistent with the range of observations for similar species and ecosystems (Harmon et al 2011, Domke et al 2011). The results confirm that declines in density drive progressive losses of biomass as SDT

move through the structure-based decay classes used nationwide by the FIA program. When these density reduction factors and net biomass changes are coupled with comprehensive live, SD, and coarse woody debris inventory through time the complete picture of carbon dynamics in California mixed conifer forests is realized.

White and red fir, Douglas fir, and ponderosa and sugar pine followed similar patterns of decomposition and density loss, losing nearly half of their live wood density. The true and Douglas firs advanced in physical decay and weathering more rapidly than pines, but retained sound bark well into decay classes 4 and 5. Standing dead pines lost bark rapidly; foraging, especially by woodpeckers and insectivorous mammals, may be a contributing factor in this trend. Pines maintained harder, more sound wood with occasional fissures and insect galleries, while firs exhibited delaminated and softening tissues. Standing dead incense cedar was remarkably resistant to changes in density, consistent with its unique chemical and physical characteristics (McDonald 1973). Past observations of incense cedar decay in the Sierra Nevada (Harmon et al. 1987) suggest that this species maintains wood density well into advanced decay stages, even in pieces of coarse woody debris on the forest floor. Furthermore, the predominant cause of death for incense cedar at this research site is physical, particularly snow damage (Schurr 2005). Accordingly, the SDT surveys did not locate a single class 1 incense cedar > 12.5 cm DBH (Table 1). Trees that enter the SD pool by breakage can advance to class 3 or 4 simply by virtue of their broken boles without any concomitant loss in density, and due to the wood's high resistance to decay, can remain intact for many years.

#### 2.4.2 Attribution of Carbon Loss: Volume Loss vs. Decay

Carbon concentration's gradual increase with decay class is likely caused by the decomposition activity of brown-rot fungi. Brown rot fungi are among the primary decomposers of wood and bark in gymnosperms but are unable to digest lignin. As decay progresses, biomass stored as digestible hemicellulose and cellulose is decomposed preferentially, with lignin-enriched tissues left behind. Because lignin has a higher C content than the other polymers that make up wood and bark, the resulting decayed matter also has greater C per unit biomass (Gilbertson 1980, Harmon et al 2013). This explanation is consistent with the pattern observed in incense cedar, a species resistant to almost all fungal onslaughts (McDonald 1973).

#### 2.4.3 Evaluation of Uncertainty

Uncertainty of DRF and other tissue characteristics was higher in middle decay classes. This higher uncertainty is likely attributable to greater heterogeneity in the range of conditions of these SDT. Trees in decay class 1 are essentially intact, while those in class 5 are broken and often thoroughly decayed. The descriptions of class 3, and to a lesser extent classes 2 and 4, encompass a wide range of structural and decay conditions. Though the decay class system is deployed across all species and regions, it was developed on the basis of a single species (Douglas fir) and is best suited to similar species (USDA Forest Service 2010, Thomas 1979). The observed uncertainty patterns likely reflect the flexibility of this five-class system and its suitability to the allometry of mixed conifer species.

The following chapter examines the longevity of SDTs in mixed conifer forests, reporting the fall rates of SDT on an annual basis. This information complements the pattern of individual

tree decay to quantify not only the degree but also the duration of carbon storage and loss by SDT.

**Table 7: Properties of Standing Dead Trees (wood and bark combined) for All Species and Decay Classes Sampled**

Species	Decay class	SD density (g/cm <sup>3</sup> )	Dead:live* density ratio	n (trees)	SD Carbon conc. (%)	Dead:live** net C ratio	n (trees)
white fir	1	0.37 (0.03)	0.92 (0.08)	5	0.51 (0.01)	0.86 (0.10)	3
white fir	2	0.35 (0.02)	0.86 (0.04)	6	0.51 (0.01)	0.84 (0.13)	2
white fir	3	0.29 (0.08)	0.72 (0.19)	4	0.51 (0.01)	0.90 (0.01)	2
white fir	4	0.22 (0.02)	0.56 (0.04)	10	0.53 (0.01)	0.60 (0.04)	9
white fir	5	0.17 (0.01)	0.43 (0.02)	3	0.54 (0.02)	0.46 (0.05)	2
red fir	1	0.38 (0.02)	1.01 (0.04)	6	0.51 (0.00)	0.97 (0.02)	4
red fir	2	0.37 (0.00)	0.98 (0.02)	3	0.51 (0.00)	1.00 (0.01)	3
red fir	4	0.40 (NA)	1.05 (NA)	1	0.52 (NA)	1.10 (NA)	1
incense cedar	2	0.28 (0.02)	0.85 (0.05)	4	0.52 (0.01)	0.84 (0.03)	3
incense cedar	3	0.29 (0.03)	0.91 (0.09)	6	0.52 (0.00)	1.02 (0.13)	3
incense cedar	4	0.30 (0.03)	0.93 (0.10)	3	0.52 (0.00)	0.97 (0.11)	3
incense cedar	5	0.30 (0.03)	0.86 (0.08)	3	0.53 (0.01)	0.91 (0.10)	3
sugar pine	1	0.34 (0.04)	0.99 (0.10)	6	0.52 (0.00)	1.09 (0.07)	2
sugar pine	2	0.26 (NA)	0.76 (NA)	1	0.52 (NA)	0.79 (NA)	1
sugar pine	3	0.26 (0.05)	0.76 (0.16)	4	0.52 (0.00)	0.79 (0.17)	4
sugar pine	4	0.26 (0.03)	0.75 (0.09)	2	0.52 (0.00)	0.78 (0.08)	2
sugar pine	5	0.19 (0.01)	0.55 (0.04)	2	0.52 (0.00)	0.56 (0.04)	2
ponderosa pine	1	0.36 (0.01)	0.96 (0.04)	3	0.53 (NA)	0.98 (NA)	1
ponderosa pine	2	0.34 (NA)	0.91 (NA)	1	0.51 (NA)	0.93 (NA)	1
ponderosa pine	3	0.34 (0.04)	0.89 (0.09)	6	0.51 (0.01)	0.98 (0.03)	3
ponderosa pine	4	0.24 (0.05)	0.63 (0.12)	8	0.53 (0.01)	0.61 (0.18)	6
ponderosa pine	5	0.20 (0.03)	0.52 (0.08)	5	0.53 (0.01)	0.55 (0.12)	4
Douglas-fir	1	0.38 (0.03)	0.85 (0.06)	4	0.52 (NA)	0.74 (NA)	1
Douglas-fir	3	0.21 (0.11)	0.48 (0.25)	2	0.51 (0.00)	0.49 (0.26)	2
Douglas-fir	4	0.26 (0.02)	0.59 (0.05)	6	0.53 (0.00)	0.62 (0.05)	6
Douglas-fir	5	0.19 (0.03)	0.43 (0.07)	3	0.56 (0.01)	0.48 (0.07)	3

\*Live density, Miles and Smith 2009. All other data this study

\*\*Live carbon concentration 50%

Values in parentheses are standard errors

**Table 8: Standing Dead Wood Properties and Bark Properties for All Species and Decay Classes Sampled**

Species	Decay class	Mean SD wood density (g/cm <sup>3</sup> )	SD wood dead:live* density ratio	n (trees)	SD wood carbon conc. (%)	n (trees)	Mean SD bark density (g/cm <sup>3</sup> )	SD bark dead:live* density ratio	n (trees)	SD bark carbon conc. (%)	n (trees)
white fir	1	0.37 (0.03)	0.86 (0.07)	5	0.5 (0.01)	3	0.66 (0.09)	1.17 (0.16)	5	0.53 (0.01)	3
white fir	2	0.35 (0.02)	0.78 (0.05)	6	0.5 (0.00)	2	0.61 (0.05)	1.09 (0.10)	6	0.54 (0.00)	2
white fir	3	0.29 (0.08)	0.68 (0.2)	4	0.51 (0.00)	2	0.48 (0.09)	0.86 (0.17)	4	0.53 (0.01)	2
white fir	4	0.22 (0.02)	0.5 (0.04)	10	0.52 (0.01)	9	0.43 (0.02)	0.77 (0.03)	10	0.56 (0.01)	9
white fir	5	0.17 (0.01)	0.38 (0.06)	3	0.53 (0.03)	2	0.32 (0.10)	0.57 (0.18)	3	0.59 (0.01)	2
red fir	1	0.38 (0.02)	1.01 (0.04)	6	0.51 (0.00)	4	0.47 (0.07)	1.07 (0.15)	6	0.52 (0.00)	4
red fir	2	0.37 (0)	0.98 (0.02)	3	0.51 (0.00)	3	0.43 (0.03)	0.98 (0.07)	3	0.52 (0.01)	3
red fir	4	0.4 (NA)	1.1 (NA)	1	0.52 (NA)	1	0.42 (NA)	0.95 (NA)	1	0.52 (NA)	1
incense cedar	2	0.28 (0.02)	0.82 (0.06)	4	0.52 (0.00)	3	0.24 (0.01)	0.97 (0.05)	4	0.53 (0.01)	3
incense cedar	3	0.29 (0.03)	0.93 (0.11)	6	0.52 (0.00)	3	0.2 (0.03)	0.82 (0.11)	6	0.52 (0.00)	3
incense cedar	4	0.3 (0.03)	0.95 (0.11)	3	0.52 (0.00)	3	0.21 (0.01)	0.85 (0.05)	3	0.52 (0.00)	3
incense cedar	5	0.3 (0.03)	0.86 (0.08)	3	0.53 (0.01)	3	0.22 (NA)	0.9 (NA)	1	0.53 (NA)	1
sugar pine	1	0.34 (0.04)	0.91 (0.12)	6	0.52 (0.00)	2	0.47 (0.04)	1.35 (0.11)	6	0.54 (0.00)	2
sugar pine	2	0.26 (NA)	0.72 (NA)	1	0.51 (NA)	1	0.34 (NA)	0.98 (NA)	1	0.53 (NA)	1
sugar pine	3	0.26 (0.05)	0.85 (0.08)	4	0.51 (0.00)	4	0.38 (0.00)	1.08 (0.01)	3	0.54 (0.00)	3
sugar pine	4	0.26 (0.03)	0.74 (0.08)	2	0.52 (0.01)	2	0.39 (NA)	1.11 (NA)	1	0.54 (NA)	1
sugar pine	5	0.19 (0.01)	0.54 (0.05)	2	0.52 (0.00)	2	0.37 (NA)	1.04 (NA)	1	0.55 (NA)	1
ponderosa pine	1	0.36 (0.01)	0.94 (0.08)	3	0.53 (NA)	1	0.38 (0.06)	1.08 (0.16)	3	0.52 (NA)	1
ponderosa pine	2	0.34 (NA)	0.93 (NA)	1	0.5 (NA)	1	0.3 (NA)	0.87 (NA)	1	0.54 (NA)	1
ponderosa pine	3	0.34 (0.04)	0.87 (0.09)	6	0.5 (0.01)	3	0.37 (0.05)	1.05 (0.15)	6	0.54 (0.01)	3
ponderosa pine	4	0.24 (0.05)	0.63 (0.12)	8	0.53 (0.01)	6	0.37 (0.04)	1.04 (0.12)	6	0.53 (0.00)	5
ponderosa pine	5	0.2 (0.03)	0.53 (0.09)	5	0.53 (0.01)	4	0.35 (0.02)	1.01 (0.06)	2	0.54 (0.00)	2
Douglas-fir	1	0.38 (0.03)	0.76 (0.06)	4	0.52 (NA)	1	0.5 (0.05)	1.14 (0.12)	4	0.53 (NA)	1
Douglas-fir	3	0.21 (0.11)	0.44 (0.25)	2	0.5 (0.00)	2	0.47 (0.05)	1.07 (0.11)	2	0.54 (0.00)	2
Douglas-fir	4	0.26 (0.02)	0.5 (0.06)	6	0.51 (0.01)	6	0.45 (0.01)	1.04 (0.02)	6	0.57 (0.01)	6
Douglas-fir	5	0.19 (0.03)	0.34 (0.05)	3	0.54 (0.02)	3	0.44 (0.00)	1 (0.01)	3	0.59 (0.01)	3

\*Live density, Miles and Smith 2009. All other data this study

Values in parentheses are standard errors

# CHAPTER 3: Fall Rates of Standing Dead Trees in California Mixed Conifer Forests

## 3.1 Introduction

...standing dead trees may result from a number of agencies, such as fire, bark beetles, tree diseases, flooding and drought. Once produced, they become of concern to foresters...

Keen 1929

Standing dead trees (SDTs) are vital but ephemeral elements of the forest. They represent the transition from living trees where entropy is actively delayed by the input of energy to coarse woody debris where the direct contact with soil microbes speeds decay. While they remain standing, these trees provide essential habitat for wildlife; they store a significant amount of carbon; and they present potential hazards (Keen 1929, Raphael and White 1984, Hilger et al. 2012).

The rate at which SDTs fall to the ground, referred to as the fall rate, directly influences forest carbon cycling. Compared to dead and downed trees that interact with the diverse community of decomposing organisms in the soil, SDTs decay much more slowly (Domke et al. 2011, Harmon et al. 2011). The carbon loss is attenuated, often for decades, while the trees remain upright. Since SDTs represent a significant carbon pool in many forests (Hilger et al. 2012), explicitly accounting for SDT dynamics will improve the estimates of greenhouse gas emissions as well as the accuracy of forest carbon modeling (Kurz et al. 2009).

Despite their importance, information on SDT fall rates remains relatively sparse (Angers et al. 2010, Parish et al. 2010) with most of the work concentrated in boreal forests. Rates can vary widely depending on the species, the size, the neighboring forest structure, and the cause of death (Morrison and Raphael 1993, Garber et al. 2005, Gibbons et al. 2008, Angers et al. 2010, Parish et al. 2010, Angers et al. 2011). A recent synthesis for North American species reports a 50-fold range in tree fall rates from a minimum of 1.2% yr<sup>-1</sup> for spruce trees in Quebec to a maximum of 54.9% yr<sup>-1</sup> for oak trees in South Carolina (Hilger et al. 2012). The dearth of information is particularly acute for California. There have been only two studies on SDT fall rates (Table 9): one in the ponderosa pine flats of the Modoc National Forest (Keen 1955) and the other in the mixed conifer/eastside pine forest of Sagehen Creek Experimental Forest (Morrison and Raphael 1993). Thus to improve greenhouse gas emission estimates from California's forests, a better understanding of the rates and drivers of fall rates for SDTs is needed.

Toward this end, the investigation capitalized on existing studies at Blodgett Forest Research Station (BFRS) and Sequoia-Kings Canyon National Parks (SEKI) to examine tree fall rates for the tree species that comprise the vast mixed conifer forests of California. Specifically, the study

developed longitudinal studies where individual trees were tracked over time. Such approaches provide the best data to quantify patterns and drivers of fall rates (Hilger et al. 2012). The objectives were to:

1. Determine the overall shape and magnitude of the SDT fall rate curves. Two common distributions have been noted: a rotated sigmoidal curve (e.g. Angers et al. 2010, Keen 1929) indicating a period of persistence immediately after a tree dies followed by a rapid increase in fall rate and an exponential curve (e.g., Raphael and Morrison 1987, Hilger et al. 2012) indicating initial high rates of tree fall followed by a tapering in later years.
2. Quantify species and size differences in SDT fall rate.
3. Compare results for SDT fall rates for California mixed conifer tree species.

## 3.2 Methods

### 3.2.1 Site Descriptions

In 1983, Blodgett Forest Research Station established a program to track the fate of standing dead trees (SDTs). Following the protocols established by Raphael and White (1984), all of the standing dead trees  $\geq 12.7$  cm DBH in Compartment 160U were inventoried and tagged. Compartment 160U (24 ha in size) is typical of the mixed conifer forest in the region. White fir, ponderosa pine, and incense cedar are the most abundant tree species. Along a low ridge within the compartment, black oak is locally common. The aspect is predominantly east-facing, with slopes variable from 5-18% and elevations ranging from 1220 to 1340 m. Standing dead trees (SDT) were initially inventoried in 1983. This dead tree inventory was updated in 1989, 1994/1995, and 2005 (Table 9). The site was extensively cut and likely burned in 1913. The forest was allowed to recover without intervention (except fire suppression) until 1963. Since then, it has been actively managed using uneven-aged treatment. Major stand entries in Compartment 160U during the inventory period include: sanitation cutting of mistletoe affected trees, 1982; group selection, 1984; single-tree selection, 1995; and thinning, 2005. Regular clearing for fuel reduction and safety near roads impacts only a small portion of the compartment.

In 1982 researchers initiated a network of permanent plots in the conifer-dominated forests of the southern Sierra Nevada to track the fate of individual trees (USGS-WERC Forest Demography Study). The focus of the demography study is to understand the processes that influence the recruitment, growth, and mortality of live trees. Toward that end, they maintain 30 large (typically 1 ha), mapped plots selected to be broadly representative of the old-growth conifer forests found in Sequoia-Kings Canyon and Yosemite National Parks. The work focused on the 21 plots that included the core species of the mixed conifer forests in the southern Sierra Nevada, namely white fir, ponderosa pine, sugar pine, incense cedar, Jeffrey pine (*Pinus jeffreyi*), red fir, and black oak. These plots spanned an elevational range from 1500 to 2576 m and most were located in SEKI. The sites were never logged and have not experienced any stand-replacing disturbances in the last several centuries. Before Euroamerican settlement, low to moderate intensity surface fires were common. Fire has been excluded since the late 1800's. Inventory data indicate that, forest-wide, neither tree density nor basal area have changed

substantially during the last two decades (van Mantgem and Stephenson 2007). So for the last 150 years, the dynamics of these forests have largely been governed by local endogenous forces.

### 3.2.2 Standing Dead Inventories

From 1983 to 2005, BFRS periodically inventoried standing dead trees in Compartment 160U to complement their overall forest monitoring program (Table 9). This effort was extended in order to lengthen the record (nearly three decades) and to obtain sufficient data for a demographic analysis of fall rates. Toward this end, the project completed a thorough census of the entire 24 ha tract in 2012. In order to efficiently search a large area, the compartment was divided into three sections. Each section was further broken down into transects 40 meters wide running East/West across the compartment using flagging to mark the boundaries. A three-person crew strategically searched the transects for standing dead and fallen trees from previous inventories as well as trees that had died since the most recent inventory in 2005. The crew members were spaced 10 meters apart along the southern edge of the East/West transect. Walking north, each crew member looked for standing and down trees until they reached the north end of the transect. The crew members then traded places and re-searched this area for trees that were missed. When the second survey was finished, they moved along the southern edge of the transect and repeated this search protocol until the section was completed. Such careful searching is necessary when tracking dead trees. For example, it can be hard to detect a recently fallen SDT that was severely decayed. Such an individual looks much like coarse woody debris.

**Table 9: Description of Sites/Data from California Conifer Forests Used in This Report**

Site	Location (county)	Forest type	Length of record (years)	Interval	Density (SDT ha <sup>-1</sup> )	N (trees)	Source
Modoc National Forest	Modoc	Mature pine stands/ beetle kill	30	1919-1949	13.2 (1919)	3,015	Keen 1929; Keen 1955
Sagehen	Nevada	Mixed conifer/ Eastside pine	10	1978-1998	16.7 (1978)	1,238	Raphael and Morrison 1987; Morrison and Raphael 1993
BFRS	El Dorado	Mixed conifer/ uneven aged management	29	1983-2012	20.0 (1983)	817	This study
SEKI	Tulare & Kern	Mixed conifer/ old-growth	31	1982-2013	31.3 (2013)	2,928	This study

Density of standing dead trees (SDTs) is reported with year of the measurement (in parentheses). Modoc NF refers to the Modoc National Forest, Sagehen to Sagehen Creek Experimental Forest, BFRS to Blodgett Forest Research Station, and SEKI to Sequoia-Kings Canyon National Parks.

Another challenge with standing dead tree inventories is that tags secured with nails are more likely to be lost as the tree decays. Thus care must be taken to distinguish new recruits to the SDT population (i.e., trees that have died since the last inventory) from trees that lost their tag. When the crew found a tagless dead tree that included brown needles or fine twigs (evidence of recent death), the tree was tagged as a new dead tree. When older standing dead trees without

tags, needles, or fine twigs were found, the crew determined if the tree was part of a previous inventory based on estimated age, size, nearby trees, and notes and attempted to reassign the original tag number. If confident, they re-tagged the tree with the old tree number. If not, it was considered as “unidentified” and assigned to a separate tag series to avoid corruption of the 2012 census inventory. Every tagged tree was measured following the original Blodgett protocol. The protocol includes measurements and categorical data describing the size, form, decay condition, estimate of the time since death, probable cause of death, and wildlife use of standing dead trees. In 2012 trees were also categorized according to FIA decay class stages (see above, USDA Forest Service 2010).

Over the course of Forest Demography Study at SEKI, 11,766 tree mortalities have been recorded (Table 10). However, live trees are the focus, and there was no explicit effort to track standing dead trees. Yet there existed the potential to capture the current status of all standing dead trees, to extend protocols to ensure SDT information is captured in the future, and to reconstruct fall dates for dead trees from the existing data.

In 2013, the authors assessed the status and decay class (as described above) of all standing dead trees in the 21 SEKI demography plots that contained core mixed conifer species. Through a combination of field forensics and database mining, they were able to assign probable fall dates for the approximately 3,000 SDTs that were  $\geq 12.7$  cm in DBH. Tree location information was central to the ability to estimate fall dates. Since every tagged tree had to be visited every year as part of the Forest Demography Study, the crew noted when standing dead trees were no longer standing so time was not wasted searching for a downed tree. Crews assembled all the location notes and comments and then searched for the first indication that a tree was no longer standing. For ambiguous cases (14.3% of the records), they recorded all potential fall dates in the order of confidence.

**Table 10: Standing Dead Tree Fall Rates for Blodgett Forest Research Station**

Species	Number of SDT	Rate Constant (k, yr <sup>-1</sup> )	Half-life (T <sub>50</sub> , years)	Annual Fall Rate (F, % yr <sup>-1</sup> )
White fir	182	0.165	4.2	15.2
Ponderosa pine	105	0.206	3.4	18.6
Sugar pine	59	0.151	4.6	14.0
Incense cedar	206	0.0855	8.2	8.1
Douglas-fir	20	0.138	5.0	12.9
Black oak	230	0.235	3.0	20.9
All species	817	0.147	4.7	13.7

The category of “All Species” includes 15 standing dead trees that could not be identified to species. Rates calculated for all individuals without normalization for tree size.

**Table 11: Standing Dead Tree Fall Rates for Sequoia-Kings Canyon National Parks**

Species	Number of SDT	Rate Constant (k, yr <sup>-1</sup> )	Half-life (T <sub>50</sub> , years)	Annual Fall Rate (F, % yr <sup>-1</sup> )
White fir	1,398	0.0618	11.2	6.0
Ponderosa pine	132	0.0957	7.2	9.1
Sugar pine	540	0.0629	11.0	6.1
Incense cedar	433	0.108	6.4	10.2
Black Oak	128	0.0671	10.3	6.5
Red fir	253	0.0637	10.9	6.2
Jeffrey pine	44	0.0333	20.8	3.3
All species	2,928	0.0708	9.8	6.8

Rates calculated for all individuals without normalization for tree size.

### 3.2.3 Standing Dead Tree Fall Rate Analysis

For BFRS, the demographic analysis employed non-parametric maximum likelihood estimators to quantify the fall rate of standing dead trees and then compared rate curves using weighted log-rank tests. Given the inventory schedule for Compartment 160U, the exact date of fall could not be determined. Census intervals ranged from 1 year (1994 to 1995) to 10 years (1995 to 2005). Thus, the data included two kinds of censoring. Some standing dead trees (n = 193) are still standing (right-censored). For the remainder, only the interval in which trees died (i.e., interval censoring) was known.

The fall rate functions of standing dead trees for different species were calculated following the recommendation of two recent reviews of the analysis of interval-censored data (Gomez et al. 2009, Fay and Shaw 2010), using Turnbull's (1976) generalization of the Kaplan-Meier estimator. To compare fall curves, the analysis used weighted log-rank tests that employ a permutation procedure when there are many samples (as in this case). Analyses were implemented in the R statistical language (R Core Team 2014) using the "interval" library provided by Fay and Shaw (2010).

For SEKI, given the regular inventory schedule (no interval censoring) and larger dataset, parametric analysis was used. The approach was to use an accelerated failure time (AFT) model to quantify fall rates. As described by Parish et al. (2010), AFT considers the distribution for time to failure (falling in the case of SDTs) conditional on specified covariables (species and size for SDTs). These covariates act multiplicatively on fall rate time. So conceptually, time to falling passes quickly or slowly depending on a tree's covariate values.

Next, the analysis developed competing models that attempt to predict fall rate as a function of species or size (as measured by DBH) or both species and size. Two function forms were

considered: exponential based on the most commonly reported empirical value for fall curves (Hilger et al. 2012) and Weibull based on the recommendation of Parish et al. (2010) for SDT analysis. To select which models were best supported by the data, differences in the Akaike Information Criterion (AIC, Burnham and Anderson 2002) were compared. The model with the lowest AIC has the best support in the data. Differences greater than 10 indicate strong support for the best model (Burnham and Anderson 2002). For comparison purposes to BFRS, the SDT fall rates at SEKI using non-parametric maximum likelihood estimators were also fit. However for all the summary metrics (described below), they calculated them with the results from best AFT model.

To compare fall rate curves, the study used half-life ( $T_{50}$ ). Half-life is defined as the time (in years) when the probability that a tree will fall equals 0.5. An equivalent definition for half-life is the time it takes for half of the standing dead trees in a cohort to fall (Hilger et al. 2012). Half-life can be expressed as an annual fall rate ( $F$ ) by first calculating the exponential decay constant ( $k$ ):

$$k = \frac{0.693}{T_{50}} \quad \text{Equation 1}$$

where  $k$  is the exponential decay constant ( $\text{yr}^{-1}$ ) and  $T_{50}$  is the half-life. This function assumes that the fall rate approximates an exponential distribution with time (Hilger et al. 2012). Annual fall rate can then be estimated as:

$$F = 100 - 100e^{-k} \quad \text{Equation 2}$$

where  $F$  is the annual fall rate ( $\% \text{ yr}^{-1}$ ) and  $k$  is the decay constant (Hilger et al. 2012). All analyses were implemented in the R statistical language (R Core Team 2014).

### 3.2.4 Incorporating Existing SDT Information

To build the most comprehensive database on SDT fall rates for California mixed conifer species, the data reported for ponderosa pine trees in the Modoc National Forest and both pine and fir trees at Sagehen Creek Experimental Forest (Table 9) was re-analyzed. Half-life for the trees in these studies was calculated, and then the decay constant and annual fall rates were estimated (as described in Equation 1 and Equation 2). SDT fall dynamics for pines in California were placed within their regional context, as defined by pine species common in the mountains of the western United States. The four California estimates were added to the database in Hilger et al. (2012) in order to plot their relative rank in the region.

## 3.3 Results

### 3.3.1 Shape and Magnitude of the Fall Rate Curve

Both the shape and magnitude of the fall rate curves differed between BFRS and SEKI (Table 9). The fall rate for all species at BFRS followed an exponential decline in the probability of standing with time since death (Figure 8, Figure 9). In contrast, at SEKI, there was a low

probability of falling for a short time immediately after death (< 5 years) followed by a steeper rate of fall with time since death (Figure 10, Figure 11, and Figure 12). Thus fall rate curves for trees at SEKI followed more of a rotated sigmoid distribution. The results from the AFT analysis confirmed this visual interpretation since the best AFT model used a Weibull distribution as opposed to an exponential distribution (see below).

Standing dead trees at BFRS fell almost twice as fast as trees at SEKI (Table 10, Table 11). On average the half-life for SDTs at BFRS was 4.7 years compared to 9.8 years at SEKI. The pattern held for species-by-species comparison with the exception of incense cedar. At BFRS, the half-life of incense cedar (8.2 years) was 28% greater than for cedar at SEKI.

### 3.3.2 Survival Rates of Standing Dead Trees by Species and Size Class

At both BFRS and SEKI, there were significant differences among species. The log-rank test rejected the null hypothesis of no species differences at BFRS ( $p < 0.001$ , Table 10). Incense cedar had the slowest fall rate at BFRS ( $8.1 \% \text{ yr}^{-1}$ ); white fir had the fastest ( $15.2 \% \text{ yr}^{-1}$ ). This approach could not explicitly test for size effects with a non-parametric approach but the pattern at BFRS suggested that larger trees stayed standing longer.

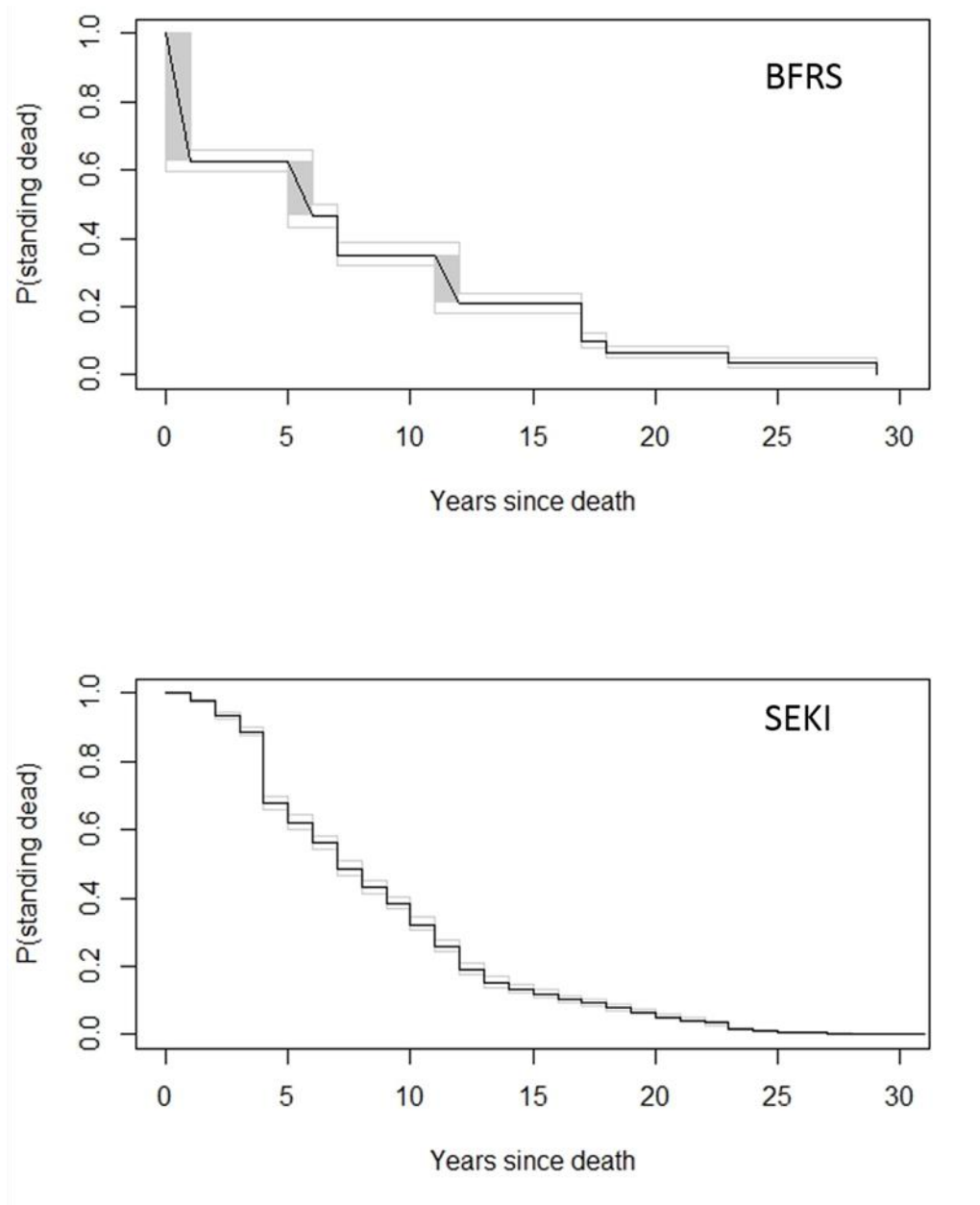
For SEKI, there was overwhelming support (the AIC of the best model was 205 points lower than the next best alternative) for the AFT model that included species, size (as measured by DBH), and the interaction of species and size. Species identity was the most important covariate determining fall rate (Table 11). In contrast to BFRS, incense cedar had the fastest fall rate at SEKI ( $6.4 \% \text{ yr}^{-1}$ ); dead Jeffrey pine trees remained standing for the longest time ( $F = 20.8 \% \text{ yr}^{-1}$ ). Fall rates also significantly decreased with increasing DBH for most species ( $p < 0.02$ ). Therefore to accurately quantify just species differences, predicted fall rates for species holding DBH constant at 40 cm were calculated (Table 12). However in absolute terms the impact of size was modest. For example, the predicted half-life for trees with a DBH = 30 cm was 9.9 years and for a tree twice that size (DBH = 60), it was 10.4 years. Thus a doubling of tree size led to a less than 6% decrease in fall rate. Also in a few species, there was a reversal of the trend – fall rate increased with increasing DBH. The most pronounced example is ponderosa pine. At a DBH = 40, the half-life for ponderosa pine is 7.7 years (Table 12). At 60 cm (a 50% increase), the half-life declined by 10% to 6.9 years.

**Table 12: Standing Dead Tree Fall Rates for Sequoia-Kings Canyon National Parks**

<b>Species</b>	<b>Number of SDT</b>	<b>Rate Constant (k, yr<sup>-1</sup>)</b>	<b>Half-life (T<sub>50</sub>, years)</b>	<b>Annual Fall Rate (F<sub>40</sub>, % yr<sup>-1</sup>)</b>
White fir	1,398	0.0624	11.1	6.1
Ponderosa pine	132	0.0904	7.7	8.6
Sugar pine	540	0.0628	11.0	6.1
Incense cedar	433	0.109	6.3	10.4
Black Oak	128	0.0667	10.4	6.5
Red fir	253	0.0621	11.2	6.0
Jeffrey pine	44	0.0336	20.6	3.3
All species	2,928	0.0688	10.1	6.7

Rates have been normalized for trees with diameters at breast height = 40 cm.

Figure 7: Standing Dead Tree Fall Rate Curves for Two Longitudinal Studies in California



Fall rate is expressed as the proportion (P) of trees still standing as a function of time since death. The grey boxes around the trend line indicate uncertainty due to interval sampling. The light grey lines represent 95% confidence intervals.

**Figure 8: Standing Dead Tree Fall Rate Curves for Three Common Species in Mixed Conifer Forests (white fir, ponderosa pine, sugar pine)**

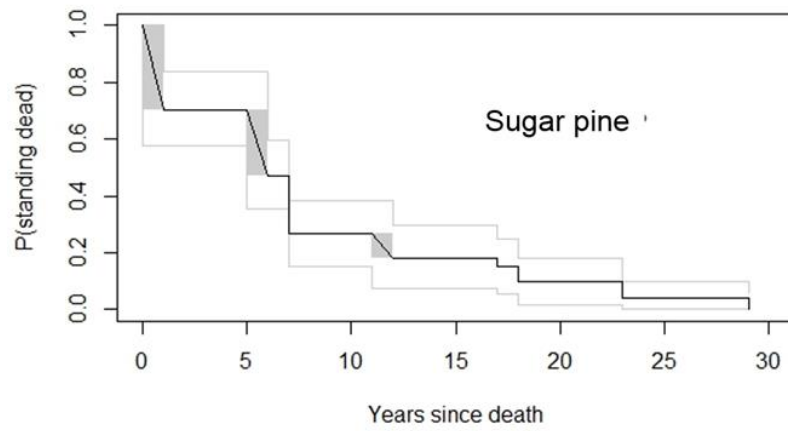
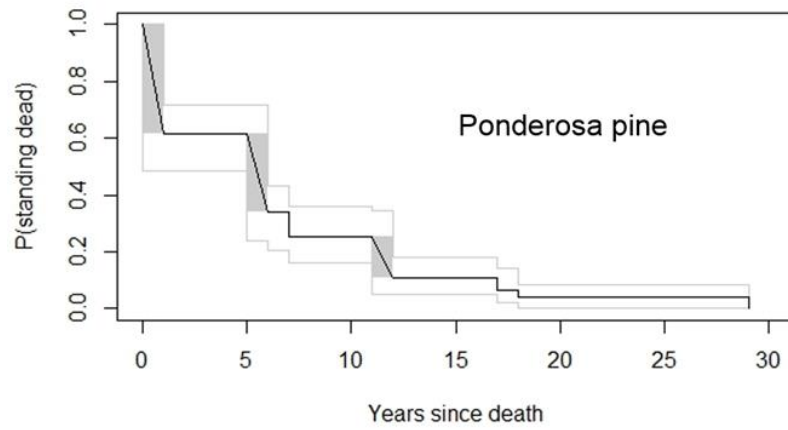
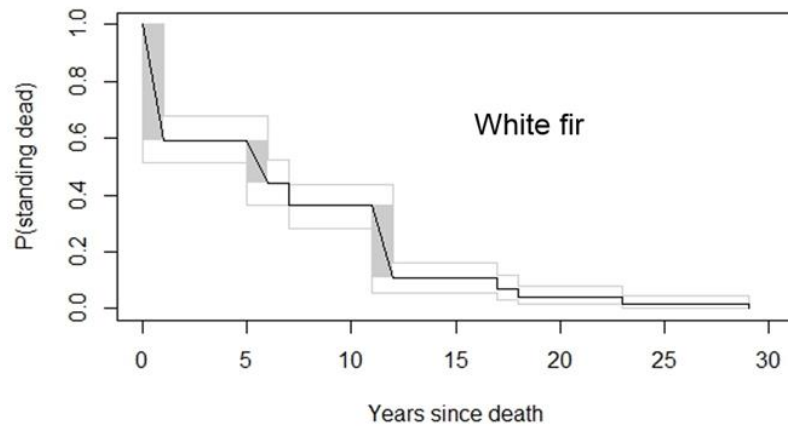
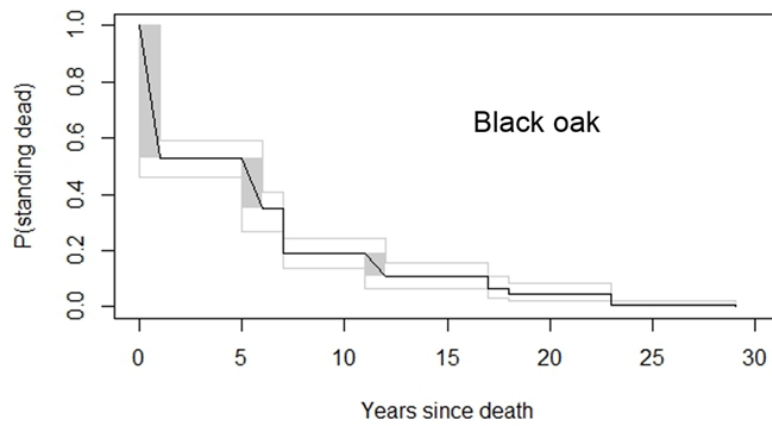
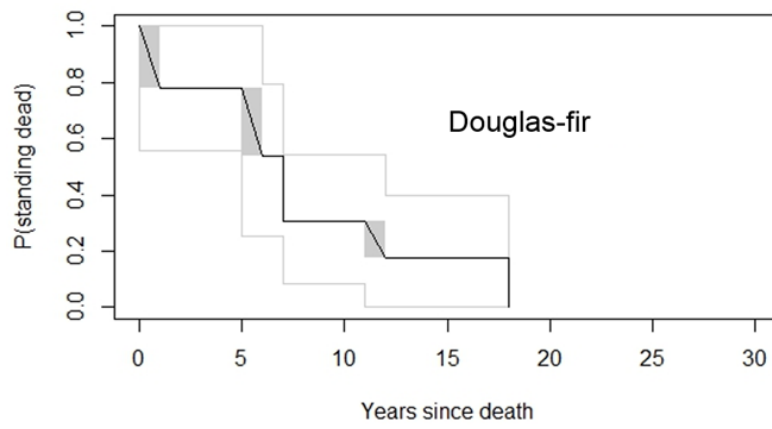
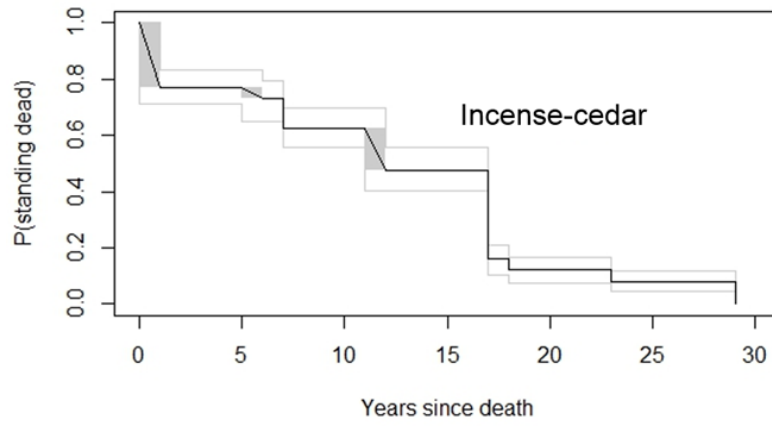


Figure 9



**Figure 9: Standing Dead Tree Fall Rate Curves for White Fir, Ponderosa Pine, and Sugar Pine Trees at SEKI**

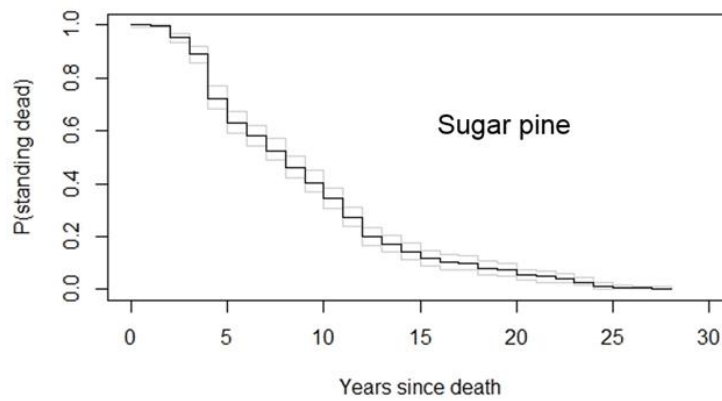
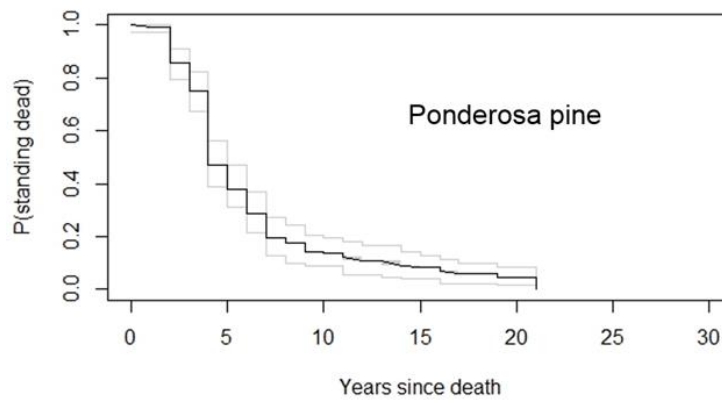
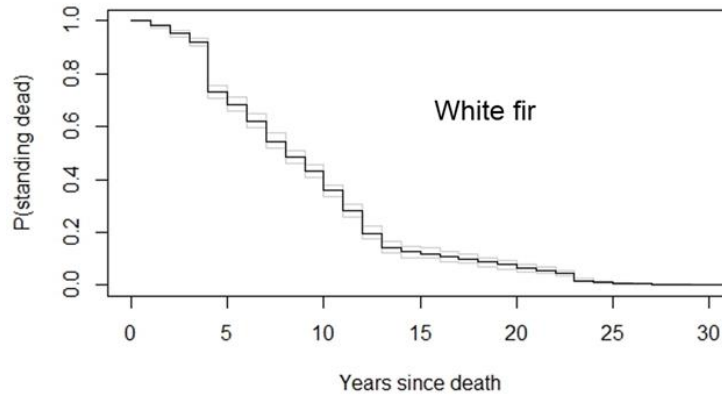


Figure 11

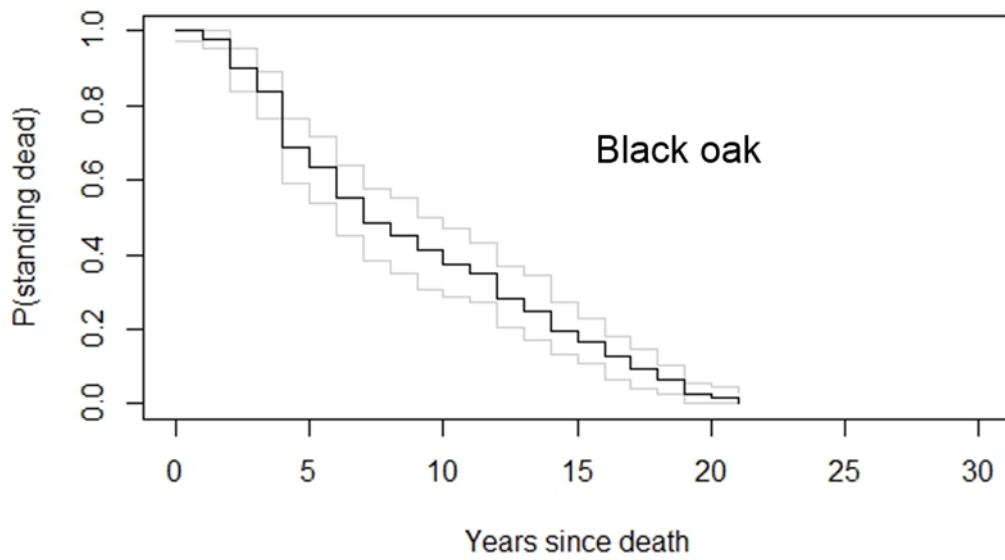
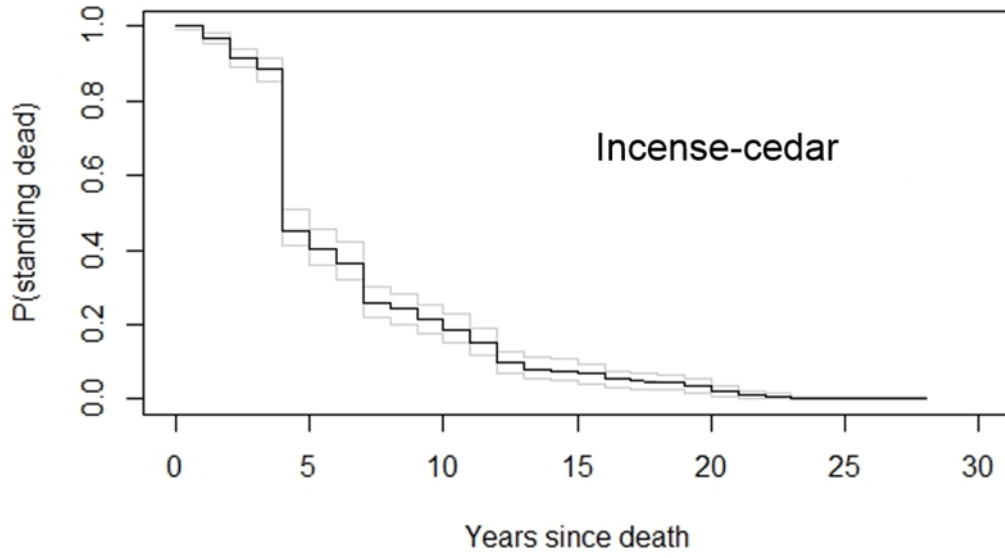
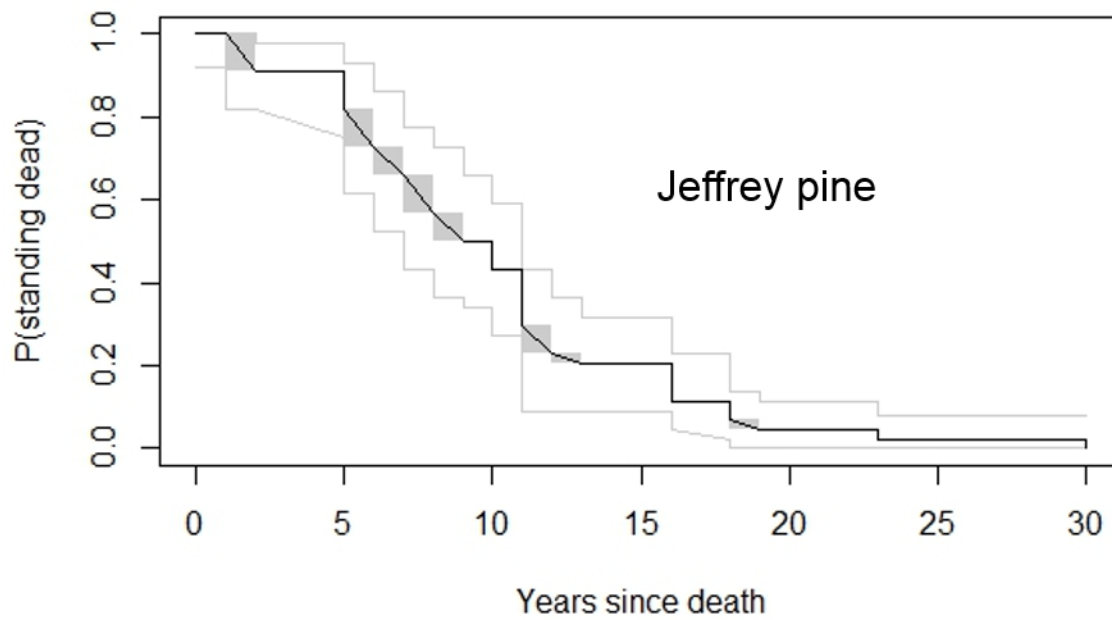
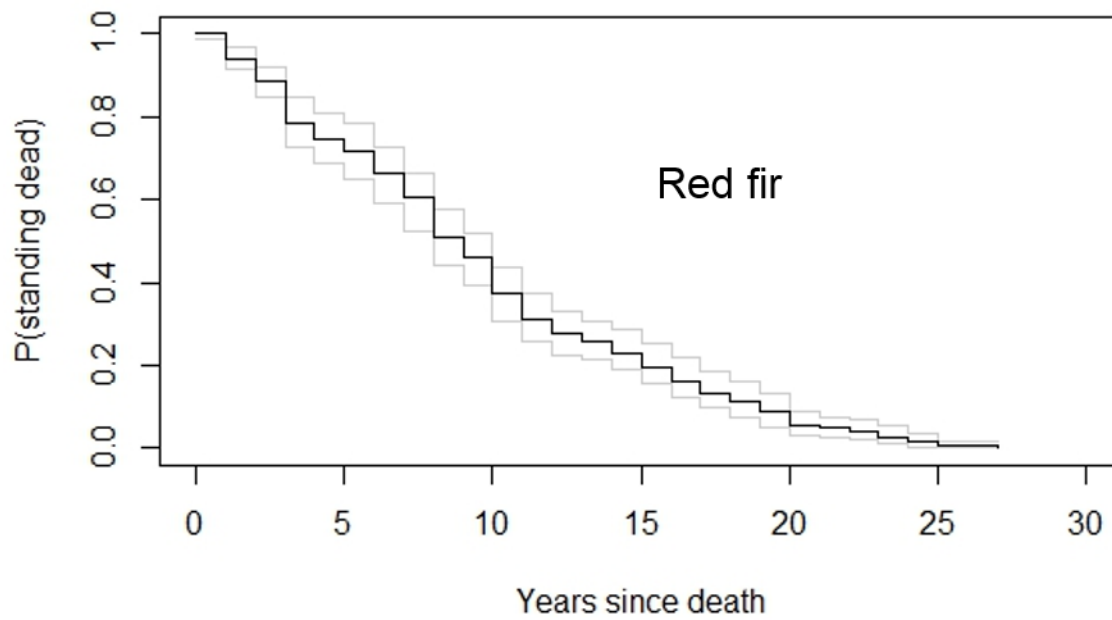


Figure 10: Standing Dead Tree Fall Rate Curves for Red Fir and Jeffrey Pine Trees at SEKI



### 3.3.3 A Comparison of SDT Fall Rates for California Mixed Conifer Tree Species

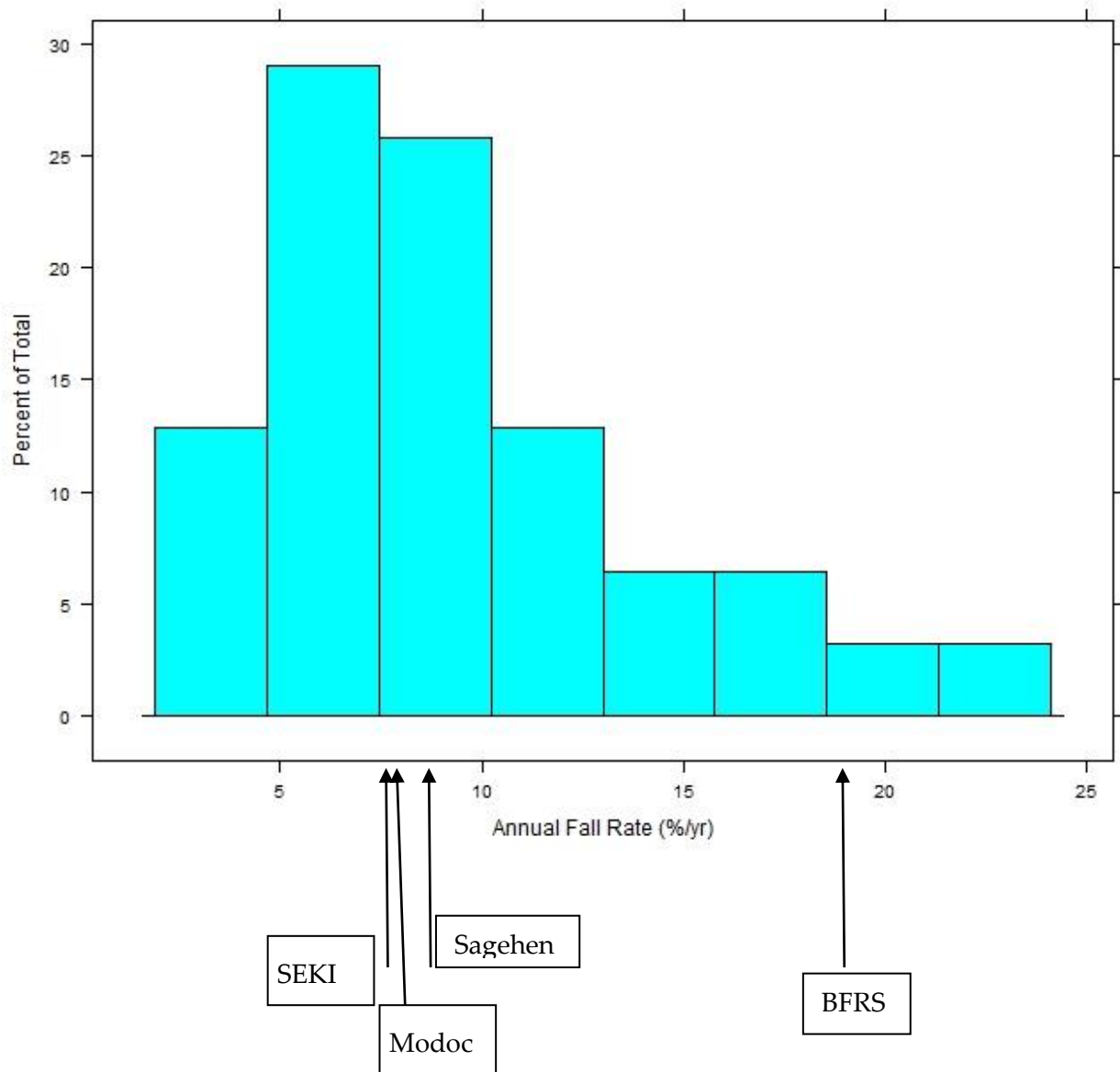
Fall rates of standing dead pine trees (largely ponderosa pine) and fir trees (largely white fir) estimated for BFRS were much faster than the other three sites (Table 13). In general, fir fell faster than pines. In comparison to pine forests in the mountains of the American West (Figure 13), annual fall rates for SDT pines in three California forests were slightly faster than the median rates. And while the rate for pines at BFRS was on the high end of the distribution, it was not the most extreme rate observed.

**Table 13: Comparison of Standing Dead Tree Fall Rates for Pine and True Fir Species in Four California Forests**

Site	Species	Rate Constant (k, yr <sup>-1</sup> )	Half-life (T <sub>50</sub> , years)	Annual Fall Rate (F, % yr <sup>-1</sup> )
Sagehen	Fir	0.128	11.1	6.1
Sagehen	Pine	0.129	7.7	8.6
Modoc NF	Pine	0.0815	8.5	7.8
SEKI	Fir	0.0621	11.2	6.0
SEKI	Pine	0.0800	8.7	7.7
BFRS	Fir	0.165	4.2	15.2
BFRS	Pine	0.206	3.4	18.6

Pines include ponderosa pine and Jeffrey pine. Fir includes white fir and red fir. Sagehen refers to Sagehen Creek Experimental Forest, Modoc NF to the Modoc National Forest, SEKI to Sequoia-Kings Canyon National Parks, and BFRS to Blodgett Forest Research Station.

**Figure 12: Distribution of Standing Dead Tree Annual Fall Rates for Pine Species in the Montane Forests of the Western United States (n = 31)**



The four sites from California (Table 13) were added to the database compiled in Hilger et al. 2012. The arrows with labels identify the California sites. Calculation methods follow Hilger et al. (2012).

### 3.4 Discussion

The SDT fall rates measured at BFRS and SEKI fall within the expected range of observations for similar species in similar forests. Added to the existing data from California and placed within the context of western mountain forests, these results provide the basis for major improvements

in estimating carbon transfers from SDTs. The results confirmed the expectation that fall rates would vary by species and size.

However BFRS and SEKI do represent opposite ends of the spectrum of forest structure and management regime for mixed conifer forests in California. The study site at BFRS is an actively managed uneven-aged stand while the SEKI plots are in a contiguous old-growth forest. Not only are individual trees at BFRS on average smaller, a factor contributing to faster fall rates, but SDTs do tend to fall faster in managed stands even when other factors are held constant (Garber et al. 2005, Gibbons et al. 2008). It is unclear exactly why this is the case – there are relatively few studies – but Garber et al. (2005) suggested it might be related to the disturbance associated with the treatments. BFRS is also a productive site that receives considerably more precipitation than SEKI (see above) and experiences less water stress (van Mantgem et al. 2007, Eitzel et al. 2013). As Keen (1955) noted, wetter sites in the pine flats had considerably faster fall rates (6.4 % yr<sup>-1</sup>) than comparable stands on drier sites (9.8 % yr<sup>-1</sup>).

Findings from both sites must be interpreted with an appropriate assessment of their robustness. In the case of BFRS, the results (e.g. Figure 8) reflect the uncertainty introduced by the varied census schedule. The interval-censoring leads to large errors in the estimates of rate of fall. In contrast, SEKI conducts annual censuses thereby avoiding issues associated with interval sampling. However until 2013, SDTs were not explicitly monitored and thus had to be reconstructed from the location notes the time of fall. There is no means to quantitatively evaluate errors in this process. However they did record ambiguities in the assignments and repeated the analysis using the alternative designations. This comparison found no tangible differences in the fall rate results with the alternative dataset. Given the nature of the reconstruction, this approach was most likely to underestimate the fall rates. Some downed trees that were obvious to researchers may not have warranted a location note to inform the crew of its status. Crews would code such a tree without an explicit note regarding its status as still being standing. However, the match between the results from SEKI and the other sites in California (Table 13) does allay potential concern about underestimates.

In the next section, this information on fall rates for SDTs will be combined with the decay reduction factors and carbon density assessment reported in Chapter 2 to quantify the potential impact on carbon storage and accounting in mixed conifer forest.

# CHAPTER 4: Improving California's Greenhouse Gas Accounting for Forest and Rangelands: Tracking Gains and Losses in the Standing Tree Carbon Pool

## 4.1 Introduction

### 4.1.1 Background

The California greenhouse gas inventory consists of annual estimates of emissions to and removals from the atmosphere for the entire state, produced by the staff of California ARB. These needs established the operational requirements for the data sources and methods used in developing the accounting approach for the forests and rangelands of California (Battles et al. 2014). The requirements included:

- Complete state coverage
- Repeat measurements over time
- Continuous data gathering in the future
- Conformity to IPCC (2006, 2013b) guidelines
- Public availability
- Moderate to fine spatial resolution for remote sensing data
- Low data processing before analysis

Given IPCC guidelines, the study partitions estimates of forest carbon into the following stocks: live tree (aboveground and total), standing dead tree, live understory vegetation, coarse woody debris, and litter. This chapter focuses on the assessment of the standing dead tree pool.

Published vegetation carbon research commonly calculates carbon stocks as the product of surface areas of land cover types, classified by satellite remote sensing (Table 14), and the carbon densities, derived from field measurements of trees and allometric equations, summed over all land cover types (e.g. Achard et al. 2004, DeFries et al. 2007, Harris et al. 2012). The number of land cover types that satellites with moderate spectral or spatial resolutions can accurately discriminate, generally five to twenty classes (e.g. Bartholomé and Belward 2005, Loveland et al. 2000), can limit the possible carbon density assignments to a few discrete values.

In contrast, other methods use Light Detection and Ranging (Lidar) or high-resolution satellites such as QuickBird, Ikonos, or WorldView (Table 14) to sense the physical dimensions of trees to which aboveground biomass directly correlates (e.g., Gonzalez et al. 2010, Saatchi et al. 2011). With these systems, forest carbon content equals the product of the area and the carbon density of each pixel, where carbon density is calculated by applying allometric equations to field measurements of individual trees and correlated to canopy height metrics estimated by Lidar or

tree crown diameter estimated by high-resolution satellite data. This method generates raster coverage of the spatial distribution of forest carbon density with continuous values.

**Table 14: Summary of Major Remote Sensing Technologies Used for Assessing Carbon Stocks**

Sensor	Scale	Platform	Mode	Detection	Access
MODIS	250 m	Satellite	Passive	36 spectral bands	Public
Landsat	30 m	Satellite	Passive	9 spectral bands	Public
QuickBird	1m	Satellite	Passive	5 spectral band	Commercial
GLAS	1 km	Satellite	Active	Light returns	Public
PALSAR	10 m	Satellite	Active	Microwave returns	Public
Lidar	<1 m	Aircraft	Active	Light returns	Commercial
Aerial photos	50 m	Aircraft	Passive	Visible spectrum	Public (NAIP)

MODIS = Moderate Resolution Imaging Spectroradiometer; GLAS = Geoscience Laser Altimeter System; PALSAR = Phased Array type L-band Synthetic Aperture Radar; Lidar = Light Detection and Ranging; NAIP = National Agriculture Imagery Program.

A recent meta-analysis of the performance of remote sensors in estimating aboveground forest biomass/carbon density (Zolkos et al. 2013) concluded that the active sensors were more accurate than the passive sensors (Table 14). In addition, various implementations of Lidar were better than any satellite-based active sensing platform. In general, the greater detail with which the tree form was resolved (e.g., height, crown width), the better the performance. However as Zolkos et al. (2013) note, the accuracy of the estimate also depended on the field measurements of tree biomass/carbon.

Estimating the carbon density of standing dead trees (SDTs) poses challenges on both fronts. They are hard to detect from above and hard to measure in the field. Landsat-based models to estimate SDT density in Washington and Oregon had poor predictive ability with performance confounded by the heterogeneity of the SDT population and the difficulty in detecting SDTs (Eskelson et al. 2012). Even with the most precise sensor (i.e., Lidar), it is difficult to distinguish live from dead trees (Pesonen et al. 2008), but recent work suggests it is possible to use synoptic measures of forest structure to predict SDT density. For example, Bater et al. (2009) were able to achieve reasonable accuracy predicting the proportional density of SDTs in an evergreen conifer forest in British Columbia using a Lidar-derived measure of the variation in vegetation height. This result adds further evidence to the potential of laser scanning technology in natural resource applications. However Lidar is currently too expensive to acquire and process to make it a viable tool in GHG accounting at regional or national scales (Zolkos et al. 2013, Battles et al. 2014). For example, extrapolating from a recent UC Berkeley/US Forest Service campaign to acquire Lidar for most of the Tahoe National Forest (3,557 km<sup>2</sup> @ \$210/km<sup>2</sup>) puts the cost of acquiring small-footprint Lidar for the forests and rangelands of California at approximately \$70M. Moreover as was noted in Chapter 2, there is limited information on the carbon density

of SDTs. Thus a comprehensive remote sensing effort would need to be matched with a similar effort on the ground.

#### 4.1.2 Problem Statement

This chapter summarizes efforts to improve the estimation of SDT carbon within the framework of the GHG inventory development funded by ARB. The inventory development called for an evaluation of geospatially explicit land use/land cover products and vegetation inventories to track biomass changes in live vegetation and then an implementation of the best available approach. As part of the Energy Commission-funded effort, this evaluation and implementation was extended to include SDTs.

## 4.2 Methods

(Note that for completeness, some methods first described in Battles et al. 2014 are included here.)

### 4.2.1 Developing GHG Accounting Approach

Despite the promise of airborne Lidar to detect both live and dead tree characteristics, the cost of its acquisition made it impractical for the ARB accounting efforts. As an alternative, other research (Baccini et al. 2008, Lefsky 2010) has demonstrated the use of laser scanning data from the ICESat satellite. ICESat Geoscience Laser Altimeter System (GLAS) global altimetry data (Abshire et al. 2005) is available for selected periods from 2003 to 2009 at 170 m spatial resolution. It is theoretically possible to take the difference between canopy elevation from GLAS and ground elevation from the United States Geological Survey (USGS) National Elevation Dataset (Gesch et al. 2002) at 30 m spatial resolution to calculate canopy height (the best predictor of live tree biomass, Gonzalez et al. 2010) and variation in forest height (the best predictor of SDT density, Bater et al. 2009). However the ICESat only made 16 passes over California, covering only a fraction of the area of the state. A complete coverage would have needed more passes and passes for multiple years. So, GLAS provided insufficient data for this work. Furthermore, GLAS would have required processing and calibration to field-measured canopy heights.

High-resolution satellite data from QuickBird, Ikonos, or WorldView is not in the public domain. This high-resolution data would also have required processing and calibration to field-measured tree crown diameters and dead tree densities. Given the expense and effort, this option was also eliminated.

The study assessed different data sources for a land cover approach. Land cover classification must use identical methods over time and data from different years must be co-registered geographically (each pixel lines up over time) to permit determination of land cover change over time. Possible land cover remote sensing options include:

- National Aeronautics and Space Administration (NASA) MODIS Land Cover Type (MCD12Q1, Friedl et al. 2010): annual 2001-2007 (available) and 2008-2010 (planned), 250 m spatial resolution, 17 land cover classes
- USGS National Land Cover Database (NLCD, Homer et al. 2007): 2001 and 2006

(available) and 2011 (in progress, but not yet available), 30 m spatial resolution, 29 land cover classes

- USGS LANDFIRE vegetation types (Ryan and Opperman 2013): 2001, 2008, 2010 (available), 2012 (planned), 30 m spatial resolution, derived from Landsat satellite data, 163 vegetation type classes in California.

Within a land cover class, it is necessary to use another variable to discriminate different levels of carbon density within a single year and growth or mortality over different years. Normalized Difference Vegetation Index (NDVI), an index related to green foliar area (Tucker 1979) and biomass (Tucker et al. 1985), and net primary productivity (NPP), a measure of annual vegetation production, are possible variables. Since none of these "green indices" directly sense the dead trees (no foliage), estimates of SDT biomass would need to rely on establishing relationships between live tree productivity or biomass and dead tree biomass. Possible vegetation level remote sensing options include:

- NASA MODIS NDVI (MOD13Q1): every 16 days from 2001 to present, 250 m spatial resolution
- USGS WELD NDVI (Roy et al. 2010): annual 2006-2010 (available) and 2011-2012 (planned), 30 m spatial resolution
- NASA MODIS NPP (MOD17A2, Running et al. 2004), every 8 days from 2000 to present, 1 km spatial resolution, vegetation production rate ( $\text{kg m}^{-2} \text{y}^{-1}$ ) calibrated to field measured biomass (Turner et al. 2006)
- USGS LANDFIRE vegetation height and cover (Ryan and Opperman 2013): 2001, 2008, 2010 (available), 2012 (planned), 30 m spatial resolution, derived from Landsat satellite data, 39 height classes and 54 vegetation cover classes in California.

After acquiring and testing different sets of land cover and vegetation level remote sensing, the advantages of LANDFIRE data became clear. LANDFIRE combines data from several sources to produce fine-grained spatial units (Rollins 2009) over which field data can be applied. In addition, the different spatial data layers can be adjusted based on what is known from the field data. If there is detailed field data (e.g., forests), carbon density assignments can be precisely resolved. If data is sparse (e.g., shrublands), generic assignments are more appropriate. When new results become available, the assignments can be improved (e.g., SDT). This matching allows a core objective to be met, namely to build a data-driven method. LANDFIRE also meets other project criteria. The USGS has completely processed and calibrated the data against field measurements, posted the data publicly, and provided three different years with plans for future releases. Moreover, the LANDFIRE variables are developed together, providing an internally consistent treatment of land cover and vegetation characteristics.

#### 4.2.2 Estimating Standing Dead Tree Carbon

LANDFIRE assigns an existing vegetation type (EVT) to each pixel that represents the species composition currently at the site. In natural ecosystems, EVT represents plant community types that tend to co-occur in environments with similar biophysical characteristics. EVT's are

hierarchical grouped into increasingly coarse units – subclass, class, order – that are consistent with the National Vegetation Classification System (NVCS, Jennings et al. 2009). The five orders used by LANDFIRE are defined by the lifeform of the dominant vegetation, namely tree (38% of the analysis area based in 2008), shrub (35%), herb (15%), no dominant vegetation (5%), and non-vegetated (6%). In addition to type, LANDFIRE assigns each pixel an existing vegetation cover (EVC) and existing vegetation height (EVH). EVC is the vertically projected percent cover of the live canopy layer for a pixel; EVH is the average height of the dominant vegetation. Both EVC and EVH are expressed as ordinal values. Together these three LANDFIRE products provide sufficient information to define relatively fine-scale biomass classes.

Given the capacity of LANDFIRE, the authors developed a carbon stock mapping method that uses a finely resolved stratify and multiply approach. By combining vegetation type, cover, and height classes, there are 100's of potential strata. The nature and number of these strata can greatly reduce within-class variation in carbon density. However these well-defined strata require sufficient data to “fill” them with estimates of carbon density.

For tree-dominated landscapes in the regional GHG accounting effort, this study relied exclusively on data from the US Forest Service (USFS) Forest Inventory and Analysis (FIA) program to calculate carbon density for biomass classes defined by LANDFIRE as tree-dominated. The FIA program is a statistically sound, national inventory of forest resources that includes a network of field plots distributed at a density of approximately one plot per 2,492 ha. Measurements in these plots (Phase 2) include nested sampling of trees (e.g., species identification, DBH, status, height, and canopy position). In the western United States, FIA plots are measured on a ten-year cycle. The fraction measured in any individual year is designed to be a representative sample of all plots in the region (Bechtold and Patterson 2005). Details of the inventory and access to the data are available online (<http://fia.fs.fed.us/>, FIADB 2011).

The FIA 2011 database for California (FIADB 2011) served as the forest inventory. This database included results from plots measured between 2001 and 2009. Exact coordinates of the location of FIA plots are not publically available. To ensure the accuracy of the biomass densities, the remote sensing lab of the USFS Region 5 provided 2001 and 2008 LANDFIRE vegetation classifications (type, subclass, class, and order), cover class and canopy height of each FIA plot in California using the exact geographic coordinates. They did not release coordinates, only the LANDFIRE values for the exact plot locations were released.

The FIA program provides plot-level estimates of key forest attributes, including those required to meet national requirements for GHG reporting (EPA 2013). Forest carbon is divided into the following pools: live tree (aboveground and total), standing dead tree, live understory vegetation, coarse woody debris, litter, and soil. Below, the logic and approach to the measurement of the SDT pool, using strata defined by LANDFIRE and informed by FIA measurements, are further explained.

This approach to estimating SDT carbon relies on the assumption that the live tree pool is the primary driver as well as the best indicator of carbon storage in forests (Fahey et al. 2010). At the most basic level, this assumption is fundamentally true for SDTs since they are created from

live trees. However it does not necessarily follow that the features of the live trees sensed by LANDFIRE (i.e., canopy cover and height) translates directly to the SDT pool. The authors tested the efficacy of predicting SDT carbon from LANDFIRE attributes by quantifying the skill with which equations estimate SDT biomass as functions of LANDFIRE canopy cover and canopy height assignments. The authors focused their efforts on the most abundant forest type in California -- the vast Sierran mixed conifer forest (21,500 km<sup>2</sup>). Specifically they compared the performance of linear, saturating, and power functions. Overall, linear combinations of height and cover proved to be the best approach. They significantly outperformed power functions based on model fits. Saturating functions were difficult to estimate given ordinal cover and height information.

Linear regressions of the general form were fit:

$$\sqrt{AG_{SDT}} = a + bEVC + cEVH + E \quad \text{Equation 3}$$

where  $AG_{SDT}$  is plot-level SDT aboveground biomass (“oven-dry”) density in Mg ha<sup>-1</sup>,  $a$  is the intercept term;  $EVC$  is the upper limit of the LANDFIRE tree cover class (e.g., cover class  $\geq 10\%$  and  $< 20\%$  was assigned a value of 20);  $EVH$  is the upper limit of the LANDFIRE tree height class;  $b$  and  $c$  are coefficients of  $EVC$  and  $EVH$ ; and  $E$  is the standard deviation of the regression.  $AG_{SDT}$  was square-root transformed to correct for positive skew in biomass distribution. Positive skew is a common feature of biological data that is routinely corrected using a square-root transformation (Sokal and Rohlf 1995).

The authors compared reduced versions of the full linear model using the Akaike’s Information Criteria (AIC). In total six models were evaluated:  $EVC$  only with an intercept term;  $EVC$  only without an intercept term;  $EVH$  only with an intercept term;  $EVH$  only without an intercept term;  $EVC$  and  $EVH$  with an intercept term (the full model, Equation. 3); and  $EVC$  and  $EVH$  without an intercept term. AIC difference values ( $\Delta AIC$ ), the difference between the AIC value of a given model ( $AIC_i$ ) and the AIC value of the best approximating model ( $AIC_{min}$ ), were used to measure the strength of evidence for each model (Burnham and Anderson 2002). Although the interpretation of  $\Delta AIC$ ’s is subjective, they provide an intuitive assessment of the strength of support for one model relative to another (Burnham and Anderson 2002). Statistical analyses were conducted in R (3.1.2).

#### 4.2.3 Incorporation of Revised Estimate (Chapter 2) of Standing Dead Tree Carbon Pools

Another objective was to incorporate improvements in the field assessment of SDT carbon into the overall GHG budget. As described in Section 2.2.1, the current FIA measurement only accounts for the volume lost as an SDT weathers. It assumes that the wood density and carbon content of an SDT remains the same as a live tree, an assumption that can lead to overestimates by as much as 40% for SDTs in the mixed conifer forest (Table 6). Using the results from Chapter 2, SDT stocks were calculated for FIA plots in the mixed conifer forest using two methods: with species-specific reduced density and carbon content according to decay class (Table 7 and without decay adjustments (FIA reported results). Then the differences across LANDFIRE cover and height classes were evaluated.

#### 4.2.4 Analytical Framework for Projecting Carbon Dynamics of Dead Trees

The death of a tree initiates the inevitable loss of stored carbon but tracking the timing of the loss is complicated. SDTs emit carbon as they decay while standing. Alternatively, when a SDT falls, its carbon is re-assigned to the coarse woody debris pool. Thus any projections of SDT carbon must account for both the weathering and decay rates (Chapter 2) as well as the fall rate (Chapter 3). As noted above, stresses related to global change have increased forest mortality rates and consequently increased the amount of carbon stored in SDTs. For example a recent analysis for the American West concludes that over the last two decades bark beetles have killed as many trees as wildfire (Hicke et al. 2013). To gain some perspective on the magnitude and timing of carbon loss to be expected from a major mortality event, the authors simulated the carbon dynamics of SDTs following an outbreak that killed 35% of the pine trees, – a realistic scenario considering that Keen (1929) reported a similar death rate for a pine stand in California. They generated a representative distribution of pine species and size classes by starting with the live tree data for all the mixed conifer plots in the FIA database. They then randomly "killed" 35% of the trees  $\geq 12.7$  cm in DBH (2,294 dead trees in 766 plots). The authors used the decay transition probabilities for pine trees 5 years and 10 years after death reported by Morrison and Raphael (1993). They then applied the correction factors that were developed (Chapter 2) to assign carbon densities by species and decay class in order to track the loss of carbon in the SDT pool over a decade.

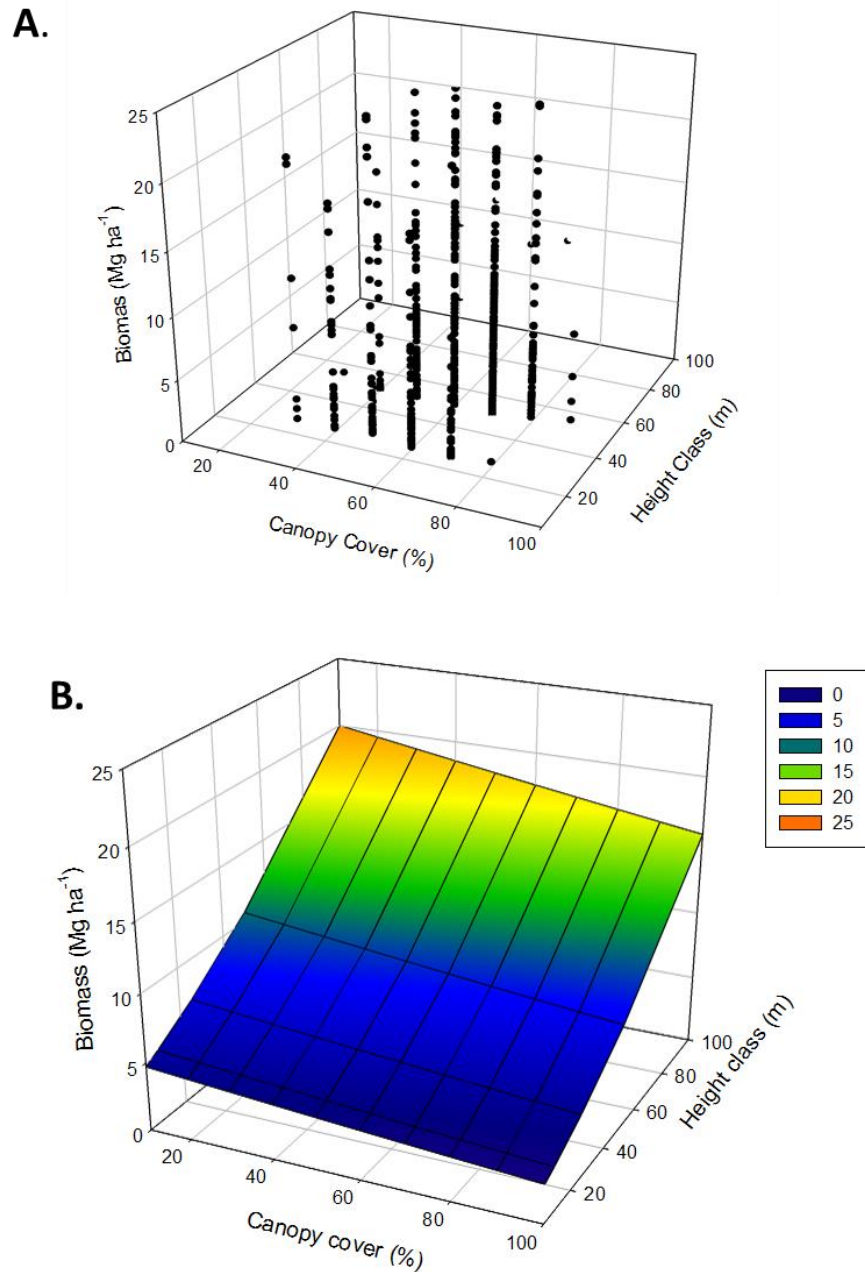
### 4.3 Results

#### 4.3.1 Performance of LANDFIRE to Detect Changes in Standing Dead Tree Biomass

Existing vegetation height (EVH) was the best LANDFIRE metric for predicting SDT biomass. For tree-dominated landscapes (i.e., forests) in general, SDT biomass significantly increased with increasing EVH. Specifically for the existing vegetation type (EVT) that was classified as Mediterranean Mesic Mixed Conifer Forest, the best model was dominated by EVH ( $p < 0.001$ ) but the existing vegetation cover (EVC) was also included in the model with the lowest AIC (Figure 14). Interestingly SDT biomass declined slightly with increasing EVC (Figure 14B). While the model captured the general trend as indicated by a significant regression model ( $p < 0.001$ ), there was a great deal of variation over individual estimates (Figure 14A) which resulted in a low goodness-of-fit ( $R^2 = 0.03$ ).

As expected, SDT biomass was significantly and positively related to live tree biomass (Figure 15,  $p < 0.001$ ). However the relationship was relatively weak ( $R^2 = 0.28$ ) particularly when live tree biomass was low. For example, plots with live tree biomass  $< 5 \text{ Mg ha}^{-1}$  had SDT biomass values that ranged from 0 to  $105 \text{ Mg ha}^{-1}$ .

**Figure 13: Standing Dead Tree Aboveground Biomass in the Mixed Conifer Forests as a Function of Canopy Cover Class and Height Class for the California Mixed Conifer Forest**



A. Estimates from 766 FIA plots. B. Statistical interpolation of results from 766 FIA plots.

#### 4.3.2 Performance of FIA in Estimating Standing Dead Tree Carbon

As documented in Chapter 2, the current FIA method systematically overestimates the carbon stored in SDTs. For the mixed conifer forest, the magnitude of the overestimate varies with the EVH and EVC (Figure 16). At the plot level, the overestimate ranged from 6% to 33% with a

median of 21%. In absolute terms, the overestimate varied from 0.3 to 4.8 Mg ha<sup>-1</sup> (median = 1.2 Mg ha<sup>-1</sup>).

**Figure 14: Relationship Between Aboveground Standing Dead Tree Carbon Density and Aboveground Live Tree Carbon Density for the 766 FIA Plots**

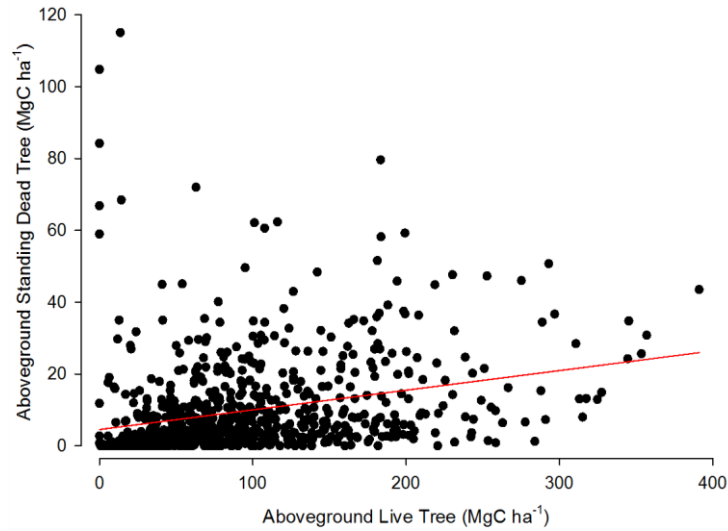
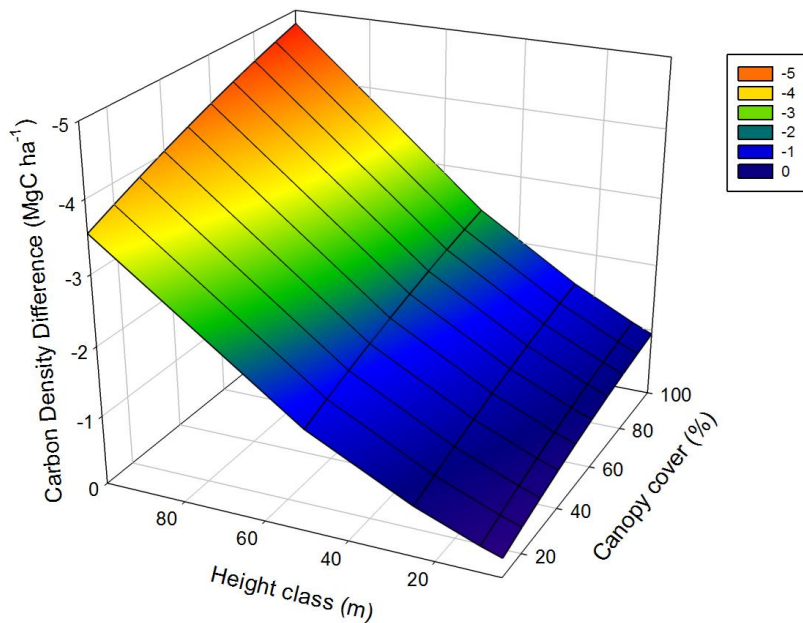


**Figure 15: Magnitude of the Overestimate in Aboveground Standing Dead Tree Carbon Density as a Function of Canopy Cover and Height Class for the California Mixed Conifer Forest**



Results are the statistical interpolation of the differences between FIA carbon density estimates and the results from Chapter 2.

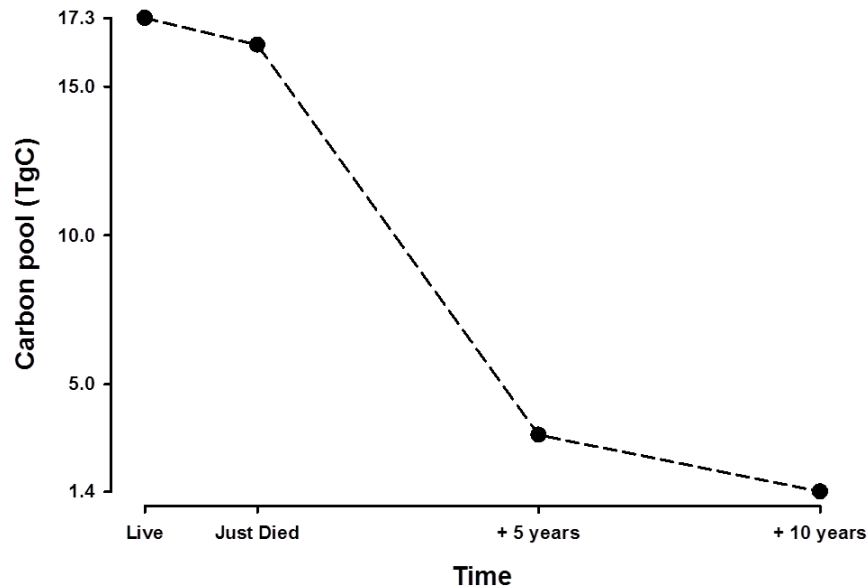
### 4.3.3 Impact of Improvements on Carbon Stocks and GHG Estimates

The regional implications of SDT decay for estimates of aboveground carbon stocks were examined by comparing the status quo estimate with an alternative, decay-adjusted estimate. SDT inventory information (volume, species, and decay class) came from 766 FIA plots in California mesic mixed conifer forests (FIADB, 2011; USGS-LANDFIRE, 2008). In these forests, SDT volume was dominated by white fir, which totaled 2801 m<sup>3</sup> and 38.5% of overall volume. Following in importance were Douglas-fir and sugar pine, which formed 17.3% and 16.7% of total SDT volume respectively. The six species included in this study (Chapter 2) accounted for 90.8% of total SDT volume (6778 of 7465 m<sup>3</sup>). In 2008, mesic mixed conifer forests had a mean live aboveground carbon density of 117 Mg ha<sup>-1</sup>, and occupied a land area of 21,500 km<sup>2</sup> in California (FIADB, 2011; USGS-LANDFIRE, 2008). This is California's single most extensive forest type and represents 5.3% of the state's total land area. The decay-adjusted carbon stock of SDTs in mesic mixed conifer forests was 9.40 Mg C ha<sup>-1</sup>, for a statewide total of 20.20 Tg. Thus, the decay-reduced SDT stock amounts to 8% of aboveground live carbon. Using the status quo approach (i.e., unadjusted) yielded a higher stock estimate: SDTs accounted for 11.16 Mg C ha<sup>-1</sup>, and a statewide total of 23.98 Tg. The difference in total carbon stock between the two estimation methods is 3.79 Tg. In summary, an estimation approach that does not account for changing net carbon density yields an 18.8% overestimate of extant SDT carbon stock.

### 4.3.4 Five and Ten-Year Projections of SDT Carbon Storage

In a mortality scenario where 35% of the pine trees were randomly killed, the percentage of SDTs in the mixed conifer increased from 13.6% of stems to 19.5% and nearly doubled the fraction of carbon stored in SDTs from 8.7% to 16.1%. In other words it was a major but not catastrophic shift in forest carbon allocation. The transition probabilities for SDT pine from Morrison and Raphael (1993) and this study's decay-adjusted estimates of SDT carbon (Chapter 2) resulted in the rapid loss/transfer of SDT carbon (Figure 17). The initial 17.3 TgC in SDT created by the simulated beetle-kill declined steeply in the 5-years following death. Most of the loss was due to treefall – nearly 60% of the SDTs fell within the first five years. During the next five years the rate of decrease declined but the loss still represented more than a 2x decline in SDT carbon (Figure 17). In summary, ten years after the end of the outbreak only 8% (1.4 TgC) of the initial SDT carbon remained in the pool.

**Figure 16: Decline in the Standing Dead Tree Carbon Pool Following a Simulated Beetle-Attack on Pine Trees in the California Mixed Conifer Forest**



## 4.4 Discussion

### 4.4.1 Implications of Dead Tree Assessment Strategies to GHG Accounting

The most recent national report of greenhouse gas emissions and sinks (US EPA 2014) relies on results from the FIA inventory to assess carbon stock changes on forest lands. Given the reliance on FIA information where the carbon density of standing dead trees is assumed to be the same as live trees, the carbon stored by decaying SDTs is overestimated. As quantified here for the mixed conifer forest in California, the extent of the overestimate can be considerable (18.8% for the SDT carbon pool). Admittedly, SDTs currently account for a relatively small fraction of forest carbon. So the overestimate is only 1% of the live+dead tree pool. However, the concern is that SDT fraction has been increasing in Californian forests and is likely to continue to increase (Section 2.1.1). Thus the magnitude of the error in GHG accounting will rise if there is a continued assumption that SDTs do not begin to decay until they fall to the ground.

This work on the decay patterns for mixed conifer trees represents a major contribution to the national effort to improve estimates of carbon stored in SDTs (Domke et al. 2011, Harmon et al. 2011). Not only did they increase the number of species with empirical estimates of SDT carbon by 40%, but they also are the first to sample across the entire decay class gradient. Harmon et al. (2011) sampled sparingly in the more severe decay classes with no measurements from the most severely decayed trees. As a first approximation, they suggest using the reduction factor for decay class 4 (Figure 2). However the results show a consistent pattern of decay (Table 6). On average, SDTs in decay class 5 had lost an additional 11% of their mass relative to class 4. Clearly the more decayed specimens present challenges, yet matching direct measurements to the inventory classification system ensures more accurate carbon accounting.

#### 4.4.2 Implications of Dead Tree Assessment to GHG Accounting Under Scenarios of Increasing Tree Mortality

Results from the beetle-kill scenario of pine trees emphasize the transient nature of the SDT carbon pool. The half-life of SDT pine was 7.7 years (Table 10). In other words, half of the stems killed in this scenario are expected to be on the ground in 7.7 years. However their projections of the carbon dynamics suggest an even faster rate of carbon transfer to the down woody debris pool (Figure 17). After only 5 years, 60% of the SDT carbon was on the ground. After 10 years, most of the trees killed were on the ground. In contrast, live canopy-sized conifers in California can live for decades (e.g., Ansley and Battles 1998) and dead logs on the ground can persist for up to 60 years (Harmon et al. 1987).

These projections of the SDT carbon loss likely overestimated the speed of the transition. In California, two modes of death are associated with severe episodes of forest mortality. Wildfires kill adult trees within hours of exposure resulting in an immediate transition from live trees to SDTs. In contrast, pest irruptions and pathogen outbreaks can take months to years to kill adult trees. The timing of the mortality event impacts timing of the transition of carbon from SDT to downed wood. In the simulation, all the trees were "killed" instantaneously and immediately started the decay process. However trees often survive for several years following an insect attack (Hicke et al. 2013). In addition, trees in a stand would die at variable rates further extending the "window of death." Nevertheless their results demonstrate that SDTs are a dynamic carbon pool with two processes to consider: *in-situ* decay and tree fall rates (Hilger et al. 2012). For mixed conifer species, the patterns of both ecological processes were quantified in order to improve GHG accounting.

# **CHAPTER 5: Conclusions**

## **5.1 Contributions of Project to Carbon Science and Ecosystem Ecology**

Growing vegetation naturally removes carbon from the atmosphere, reducing the magnitude of climate change. Conversely, deforestation, wildfire, and other agents of tree mortality emit carbon to the atmosphere, exacerbating climate change. Determining the balance between ecosystem carbon emissions to the atmosphere and removals from the atmosphere is essential for tracking the role of ecosystems in climate change (Ciais et al. 2013).

This project addressed the carbon consequences when trees die standing. SDTs are emitters but the course and rate at which the stored carbon is lost to the atmosphere depends on two processes: the rate of decay while standing and the rate at which trees fall. This project explored these rates in the vast mixed conifer forests of the Sierra Nevada.

The trend of a progressive loss of biomass of SDTs in the mixed conifer forest is consistent with observations for other conifer trees in temperate forests (Harmon et al. 2011, Domke et al. 2011). Steep declines in wood density with increasing decay class offset the small increases in carbon content. The net result was as much as a 60% reduction in carbon storage for the most severely decayed SDTs compared to a live tree of the same volume. These results represent the first measurement of SDT carbon content in California. Moreover, this project was the first to extend the field sampling to the most decayed tree classes in the US Forest Service's Forest Inventory and Analysis monitoring program, thereby providing empirical support to a projected trend in carbon decline with decay class (Harmon et al. 2011).

The measured tree-fall rates for SDTs also fell within the range of observations for conifer species in temperate forests. In general, dead fir trees in the mixed conifer forest remained standing longer than dead pine trees, suggesting a genus level variation in wood density and decay resistance. In terms of site and management effects, there was a sharp difference in the timing of fall-rates between the younger managed forest and the old-growth reserve forest. Even after accounting for differences in size, SDTs fell about twice as fast in the managed forest. Results from this study double the amount of data on fall-rates for conifer trees in California.

## **5.2 Impact of Enhancements on Current GHG Monitoring in California**

Determining more precisely the carbon balance of California ecosystems is essential for implementing climate change policy because the State of California is one of the few jurisdictions in the world to enact mandatory greenhouse gas emissions reductions. The California Global Warming Solutions Act of 2006, AB 32, sets a goal of reducing state emissions to 1990 levels by 2020. The state set a target for ecosystems (primarily forest ecosystems) of no net loss of carbon by 2020 (ARB 2008). To measure progress toward this goal, the state has identified the minimization of uncertainties in ecosystem carbon estimates as a priority for the

state greenhouse gas inventory (ARB 2014). This study directly addresses a known uncertainty in the forest carbon assessment: namely the dearth of knowledge about the carbon emission rate of standing dead trees. Results for the mixed conifer forests suggest that incorporating species-specific and decay-class specific density reduction factors into the forest carbon assessment will improve the accuracy of the SDT stock estimate by 23%. This refinement translates into a 1.7% improvement in the estimate of the carbon stored in the aboveground tree component (i.e., live and standing dead trees) of the mixed conifer forest.

## 5.3 Future Directions and Next Steps

### 5.3.1 Rationale for Efforts to Enhance Understanding of Dead Tree Carbon Ecology

As a direct result of well-documented increases in forest morbidity and mortality, SDTs are becoming ever more important players in forest carbon dynamics. Increasing climatic stress, chronic and widespread air pollution, and pest outbreaks have fueled forest die-offs worldwide, with broad implications for ecosystem structure and function (Allen et al. 2010, Hicke et al. 2013). In the North American West, increases in mortality are widely attributable to warming and increased water deficits (van Mantgem et al. 2009), often in combination with irruptions of bark beetles (Bentz et al. 2009). Across the western US from 1997 to 2010, bark beetles killed trees containing 2-24 teragrams (Tg) carbon year<sup>-1</sup> on over 5 million ha (Hicke et al. 2013). Similarly, mountain pine beetle related mortality in British Columbia has caused forests there to become a net source of carbon, a shift that may last for decades into the future (Kurz et al. 2008). In Sierra Nevada old growth forests, tree mortality rates across all taxonomic groups have more than doubled in recent years (van Mantgem and Stephenson 2007). Climate change projections and emissions trends indicate a future of exacerbated environmental stress both for California's forests (Battles et al. 2009, Moser et al. 2009, Panek et al. 2013) and forests throughout the western United States (Allen et al. 2010, IPCC 2007). High exposure to ozone pollution that contributes to tree stress and death is already the norm in parts of California and is expected for nearly 50% of global forests within this century (Fowler et al. 1999, Panek et al. 2013). Elevated tree mortality will contribute to a growing deadwood carbon pool and result in regional increases in GHG emissions. Increasing mortality may transform impacted forest ecosystems from effective sinks to significant sources of atmospheric C and N greenhouse gas compounds (Kurz et al. 2008).

In continental US and Canada forests, SDTs currently form between 5% and 35% of aboveground forest biomass (Aakala et al. 2008, Vanderwel et al. 2008). Western US conifer forests are at the upper end of this range; for these forest types, field-based estimates range from 2.4 to 7.2 Mg carbon ha<sup>-1</sup> (Woodall et al. 2012). In California mixed conifer forests, SDTs contain an average of 9.5 Mg carbon ha<sup>-1</sup>, or, 20.5 Tg (Battles et al. 2014). Current abundance of standing and down dead wood in California forests form a background mortality rate of around 1% (van Mantgem et al. 2009). This rate is expected to continue climbing, heightening the abundance of SDTs and the importance accurate SDTs biometrics.

Forest biomass pools and fluxes are also the subject of regulation and policy at state, federal, and international levels of government. Notably, SDTs form one of five forest sector carbon pools included in the U.S. National Greenhouse Gas Inventory (NGHGI) (EPA 2013). The

NGHGI is in turn used for reporting to international bodies including the Intergovernmental Panel on Climate Change and United Nations (IPCC 2006, UN 1992). At the state level, California's Global Warming Solutions Act has created demand for an accurate estimation of all sectors and phases of carbon dynamics, including SDTs (ARB 2008).

Current trends suggest that carbon stored in SDTs will continue to increase. And yet, the empirical basis for assessing carbon transfer rates in SDTs remains sparse. Work to date indicates that rates vary by species, by decay class, and by site. Clearly more information is needed at both the state and national level to capture this variation. Moreover, a product of this study is a detailed description of a robust methodology to measure carbon transfer rates in SDTs. As a result of this study, the means now exist to accomplish the needed broad-based survey of dead tree carbon storage.

### 5.3.2 Limitations of LANDFIRE

The approach developed by this project to remotely sense SDT abundance relies on the functional relationship between live and dead trees. Changes in LANDFIRE cover and height classes do capture the major gradient in SDT carbon (Figure 14) but the assignment of specific biomass values based on live tree biomass is imprecise (Figure 15). As yet, there exists no cost effective remote technology that can sense individual SDTs. The current best approaches rely on remote sensing of change in the live vegetation characteristics to infer changes in the dead tree carbon pool (e.g., Hicke et al. 2013).

### 5.3.3 Immediate Next Steps

The next step is to incorporate the decay reduction factors developed for SDTs in Chapter 2 to the stock-change assessment developed for the ARB (Battles et al. 2014). For forests and other working lands, Battles et al. (2014) delivered to ARB an operational method consistent with the atmospheric flow approach currently used by ARB that would allow ARB to repeat estimates of vegetation carbon and GHG emissions/removals in the future. For species not included in this study, Harmon et al. (2011) suggest using indices of SDT decay reduction factors based on the more extensive data on decay rates of dead and downed trees. By combining results from this study with the indices from Harmon et al. (2011), the next iteration of the ARB stock-change assessment will include a more accurate estimate of carbon emissions and removals from the standing dead tree pool.

### 5.3.4 Promise of LandTrendr: A Novel Technology Designed to Detect Forest Disturbance

One promising technology for detecting the carbon stored in standing dead trees involves a novel approach for processing images obtained from the Landsat Thematic Mapper. The LandTrendr algorithms (Landsat based detection of trends in disturbance and recovery) simplify the spectral information from Landsat images in order to process individual pixels at an annual time step (Kennedy et al. 2010). The spectral information is systematically reduced to an index that captures disturbance events. These signals of disturbances can in turn be linked to plot-level estimates of SDT basal area (Hudak et al. 2013).

## 5.4 Benefits to California

Results from this project directly support the ARB and its charge to implement AB 32. In addition, by improving the assessment of carbon stocks consistent with IPCC guidelines, the project supports efforts by the California Climate Action Registry to collect data on facility-level and entity-wide greenhouse gas emissions per the 2005 Integrated Energy Policy Report. Results reported here suggest that the forest sector sequesters less carbon than was previously estimated in standing dead trees. Thus, these results have implications for calculating the benefit of forest carbon offset projects. The study turns field-based information into knowledge useful for environmental policymaking, planning by energy utility operators and other regulated industries, and investment in ecosystem services markets. In addition, the analysis of new field data on tree fall rates and its synthesis with existing information provides a practical guide to estimating the timing of tree fall following tree death. Not only do these species and size specific tree fall rates inform carbon transfer dynamics but also they can be used to estimate the risks posed by recently dead trees near power lines.

## GLOSSARY

<b>Term or Acronym</b>	<b>Definition</b>
AIC	Akaike Information Criterion
AFT	accelerated failure time
ARB	Air Resources Board
BFRS	Blodgett Forest Research Station
C	Carbon
DBH	Tree diameter at breast height, 1.37 meters or 4.5 feet above ground
DD	Down dead
DRF	Density reduction factor. Ratio of average standing dead density to live or undecayed density with equal volume assumed.
Energy Commission	California Energy Commission
US EPA	United States Environmental Protection Agency
EVC	Existing vegetation cover
EVH	Existing vegetation height
EVT	Existing vegetation type
FIA	Forest Inventory and Analysis Program
GHG	Greenhouse Gas
GLAS	Geoscience Laser Altimeter System
IPCC	Intergovernmental Panel on Climate Change
LandTrendr	Landsat based detection of trends in disturbance and recovery
Lidar	Light Detection and Ranging
MODIS	Moderate Resolution Imaging Spectroradiometer
NAIP	National Agriculture Imagery Program
NASA	National Aeronautics and Space Administration
NDVI	Normalized Difference Vegetation Index
NPP	Net Primary Productivity
NPS	National Park Service
NVCS	National Vegetation Classification System
PALSAR	Phased Array type L-band Synthetic Aperture Radar
SD	Standard deviation
SD, SDT	Standing dead, standing dead tree
SE	Standard Error
SEKI	Sequoia and Kings Canyon National Parks
SLA	Structural Loss Adjustment
USDA	United States Department of Agriculture
USFS	
USGS-WERC	United States Geological Survey Western Ecological Research Center
WELD	Web-enabled Landsat Data

<b>Species abbreviation</b>	<b>Common name, scientific name</b>
ABCO	white fir, <i>Abies concolor</i> var. <i>lowiana</i> (Gordon) Lindley ex Hildebrand.
ABMA	red fir, <i>Abies magnifica</i> , A. Murray.
CADE	incense cedar, <i>Calocedrus decurrens</i> , (Torrey) Florin.
PILA	sugar pine, <i>Pinus lambertiana</i> , Douglas.
PIPO	ponderosa pine, <i>Pinus ponderosa</i> , Douglas ex Lawson.
PSME	Douglas fir, <i>Pseudotsuga menziesii</i> , (Mirbel) Franco.

## REFERENCES

- Aakala, T., T. Kuuluvainen, S. Gauthier, L. De Grandpre. 2008. Standing dead trees and their decay-class dynamics in the northeastern boreal old-growth forest of Quebec. *Forest Ecology and Management* 255:410-420.
- Aalde, H., P. Gonzalez, M. Gytarsky, T. Krug, W.A. Kurz, S. Ogle, J. Raison, D. Schoene, N.H. Ravindranath, N.G. Elhassan, L.S. Heath, N. Higuchi, S. Kainja, M. Matsumoto, M.J.S. Sánchez, and Z. Somogyi. 2006. Forest Land. In Intergovernmental Panel on Climate Change. National Greenhouse Gas Inventory Guidelines. Institute for Global Environmental Strategies, Hayama, Japan.
- Abshire, J.B., X. Sun, H. Riris, J.M. Sirota, J.F. McGarry, S. Palm, D. Yi, and P. Liiva. 2005. Geoscience Laser Altimeter System (GLAS) on the ICESat Mission: On-orbit measurement performance. *Geophysical Research Letters* 32: L21S02. doi:10.1029/2005GL024028.
- Achard, F., H.D. Eva, P. Mayaux, H.J. Stibig, and A. Belward. 2004. Improved estimates of net carbon emissions from land cover change in the tropics for the 1990s. *Global Biogeochemical Cycles* 18: GB2008. 10.1029/2003GB002142.
- Air Resources Board, 2014. California's 2000-2012 Greenhouse Gas Emissions Inventory Technical Support Document. State of California Environmental Protection Agency Air Resources Board, Air Quality Planning and Science Division, May 2014. Available: [http://www.arb.ca.gov/cc/inventory/doc/methods\\_00-12/ghg\\_inventory\\_00-12\\_technical\\_support\\_document.pdf](http://www.arb.ca.gov/cc/inventory/doc/methods_00-12/ghg_inventory_00-12_technical_support_document.pdf)
- Allen, C. D., A. K. Macalady, H. Chenchouni, D. Bachelet, N. McDowell, M. Vennetier, T. Kitzberger, A. Rigling, D. D. Breshears, E. H. Hogg, P. Gonzalez, R. Fensham, Z. Zhang, J. Castro, N. Demidova, J. H. Lim, G. Allard, S. W. Running, A. Semerci, and N. Cobb. 2010. A global overview of drought and heat-induced tree mortality reveals emerging climate change risks for forests. *Forest Ecology and Management* 259:660-684.
- Angers, V. A., P. Drapeau and Y. Bergeron. 2010. Snag degradation pathways of four North American boreal tree species. *Forest Ecology and Management* 259: 246-256.
- Angers, V. A., S. Gauthier, P. Drapeau, K. Jayen, and Y. Bergeron. 2011. Tree mortality and snag dynamics in North American boreal tree species after a wildfire: a long-term study. *International Journal of Wildland Fire* 20:751-763.
- Ansley, J.S. and J.J. Battles. 1998. Forest composition, structure, and change in an old-growth mixed conifer forest in the northern Sierra Nevada. *Journal of the Torrey Botanical Society* 125: 297-308.
- Association of Analytical Communities. 2006. Official Method 972.43. Microchemical Determination of Carbon, Hydrogen, and Nitrogen, Automated Method, in Official Methods of Analysis of AOAC International, 18th edition, Revision 1, 2006. Chapter 12, pp.

5-6, AOAC International, Gaithersburg, MD.

- Baccini, A., N Laporte, S.J. Goetz, M. Sun, and H. Dong. 2008. A first map of tropical Africa's above-ground biomass derived from satellite imagery. *Environmental Research Letters* 3: 045011. doi: 10.1088/1748-9326/3/4/045011.
- Bartholomé, E. and A.S. Belward. 2005. GLC2000: A new approach to global land cover mapping from Earth observation data. *Intl Journal of Remote Sensing* 26: 1959-1977.
- Bater, C,W,, N.C. Coops, S.E. Gergel, V, LeMay, and D, Collins. 2009. Estimation of standing dead tree class distributions in northwest coastal forests using lidar remote sensing. *Canadian Journal of Forest Research* 39:1080-1091.
- Battles, J. J., P. Gonzalez, T. Robards, B. M. Collins, and D. S. Saah. 2014. Final Report: California Forest and Rangeland Greenhouse Gas Inventory Development. California Air Resources Board Agreement 10-778. <http://www.arb.ca.gov/research/apr/past/10-778.pdf>
- Battles, J. J., T. Robards, A. Das, and W. Stewart. 2009. Projecting climate change impacts on forest growth and yield for California's Sierran mixed conifer forests. California Climate Change Center, March 2009. CEC-500-2009-047-D; prepared for the California Energy Commission.
- Battles, J. J., D. S. Saah, T. Robards, S. Cousins, R. A. York, D. Larson. 2013. A natural resource condition assessment for Sequoia and Kings Canyon National Parks: Appendix 12 – intact forests. Natural Resource Report NPS/SEKI/NRR—2013/665.12. National Park Service, Fort Collins, Colorado.
- Bechtold, W.A. and P.L. Patterson. 2005. The enhanced forest inventory and analysis program: national sampling design and estimation procedures. Gen. Tech. Rep. SRS-80. Asheville, NC: U.S. Department of Agriculture, Forest Service, Southern Research Station. 85 p.
- Bentz, B. J. , J. Régnière, C. J. Fettig, E. M. Hansen, J. L. Hayes, J. A. Hicke, R. G. Kelsey, J. F. Negrón, and S. J. Seybold. 2010. Climate change and bark beetles of the western United States and Canada: Direct and indirect effects. *BioScience* 60(8):602– 613.
- Bergman, R. 2010. Drying and Control of Moisture Content and Dimensional Changes. Chapter 13 in *Forest Products Laboratory (Ross, R. J.) 2010. Wood handbook : wood as an engineering material. Centennial ed. General Technical Report FPL ; GTR-190. Madison, WI : U.S. Dept. of Agriculture, Forest Service, 2010: 1 v*
- Biging, G. S. 1984. Taper Equations for Second-Growth Mixed Conifers of Northern California. *Forest Science* 30:1103-1117.
- Blodgett Forest Research Station. 2008. Blodgett Forest Inventory Guide Revision of July 15, 2008.

- Brown, S., T. Pearson, A. Dushku, J. Kadyzewski, and Y. Qi. 2004. Baseline Greenhouse Gas Emissions and Removals for Forest, Range, and Agricultural Lands in California. Winrock International, for the California Energy Commission, PIER Energy-Related Environmental Research. 500-04-069F. [http://www.energy.ca.gov/pier/project\\_reports/500-04-069.html](http://www.energy.ca.gov/pier/project_reports/500-04-069.html)
- Bunnell, F. L., and I. Houde. 2010. Down wood and biodiversity — implications to forest practices. *Environmental Reviews* 18:397-421.
- Burnham, K. P. and D. R. Anderson. 2002. Model selection and multimodel inference: a practical information-theoretic approach. Springer-Verlag, New York.
- California Air Resources Board (ARB), 2008. Climate Change Scoping Plan. ARB, Sacramento, California.
- California Air Resources Board (ARB), 2014. First Update to California's Climate Change Scoping Plan. ARB, Sacramento, California.
- Caprio, A.C., and T.W. Swetnam. 1993. Historic fire regimes along an elevational gradient on the west slope of the Sierra Nevada, California. USDA Forest Service Gen. Tech. Rep. INT-GTR-320.
- Ciais, P., Sabine, C., Bala, G., Bopp, L., Brovkin, V., Canadell, J., Chhabra, A., DeFries, R., Galloway, J., Heimann, M., Jones, C., Le Quéré, C., Myneni, R.B., Piao, S., Thornton, P., 2013. Carbon and other biogeochemical cycles, in: Stocker, T.F., Qin, D., Plattner, G.K., Tignor, M., Allen, S.K., Boschung, J., Nauels, A., Xia, Y., Bex, V., Midgley, P.M. (Eds.), *Climate Change 2013: The Physical Science Basis. Contribution of Working Group I to the Fifth Assessment Report of the Intergovernmental Panel on Climate Change*. Cambridge University Press, Cambridge, UK and New York, New York, USA.
- Das, A., Battles, J., Stephenson, N., van Mantgem, P., 2007. The relationship between tree growth patterns and likelihood of mortality: a study of two tree species in the Sierra Nevada. *Canadian Journal of Forest Research* 37, 580-597.
- DeFries, R., F. Achard, S. Brown, M. Herold, D. Murdiyarso, B. Schlamadinger, and C. de Souza. 2007. Earth observations for estimating greenhouse gas emissions from deforestation in developing countries. *Environmental Science and Policy* 10: 385-394.
- Domke, G.M., C.W. Woodall and J.E. Smith. 2011. Accounting for density reduction and structural loss in standing dead trees: implications for forest biomass and carbon stock estimates in the United States. *Carbon Balance and Management* 6: 14.
- EPA. 2013. Inventory of U.S. Greenhouse Gas Emissions and Sinks: 1990-2011. Available at <http://www.epa.gov/climatechange/emissions/usinventoryreport.html>
- Eitzel, M., J.J. Battles, R.A. York, J. Knape, and P. de Valpine. 2013. Estimating tree growth models from complex forest monitoring data. *Ecological Applications* 23: 1288-1296.

- Eskelson, B. N. I., H. Temesgen, and J. C. Hagar. 2012. A comparison of selected parametric and imputation methods for estimating snag density and snag quality attributes. *Forest Ecology and Management* 272: 26-34.
- Fahey, T.J., P.B. Woodbury, J.J. Battles, S. Ollinger, S. Hamburg, C. Woodall, and C. Goodale. 2010. Forest Carbon: Ecology, Management and Policy. *Frontiers in Ecology and the Environment* 8: 245-252.
- Fay, M.P., and Shaw, P.A. 2010. Exact and asymptotic weighted logrank tests for interval censored data: The interval R package. *Journal of Statistical Software* 36:1-34.
- Forest Products Laboratory. 2010. Wood handbook—Wood as an engineering material. General Technical Report FPL-GTR-190. Madison, WI: U.S. Department of Agriculture, Forest Service, Forest Products Laboratory. Robert Ross, Editor. 508 p.
- Forest Inventory and Analysis Database (FIADB), 2011. FIADB 5.1 (data for California through 2009, created November 23, 2011). Available online: <http://apps.fs.fed.us/fiadb-downloads/datamart.html>.
- Fowler, D., J. Cape, M. Coyle, C. Flechard, J. Kuylenstierna, K. Hicks, D. Derwent, C. Johnson, and D. Stevenson. 1999. The global exposure of forests to air pollutants. *Water Air and Soil Pollution* 116:5-32.
- Friedl, M.A., D. Sulla-Menashe, B. Tan, A. Schneider, N. Ramankutty, A. Sibley, X. Huang. 2010. MODIS Collection 5 global land cover: Algorithm refinements and characterization of new datasets. *Remote Sensing of Environment* 114: 168-182.
- Friend, A. D., W. Lucht, T. T. Rademacher, R. Keribin, R. Betts, P. Cadule, P. Ciais, D. B. Clark, R. Dankers, P. D. Falloon, A. Ito, R. Kahana, A. Kleidon, M. R. Lomas, K. Nishina, S. Ostberg, R. Pavlick, P. Peylin, S. Schaphoff, N. Vuichard, L. Warszawski, A. Wiltshire, and F. I. Woodward. 2014. Carbon residence time dominates uncertainty in terrestrial vegetation responses to future climate and atmospheric CO<sub>2</sub>. *Proceedings of the National Academy of Sciences* 111:3280-3285.
- Garber, S. M., J.P. Brown, D.S. Wilson, D. A., Maguire and L.S. Heath, L. S. 2005. Snag longevity under alternative silvicultural regimes in mixed-species forests of central Maine. *Canadian Journal of Forest Research* 35: 787-796.
- Gesch, D., Oimoen, M., Greenlee, S., Nelson, C., Steuck, M., and Tyler, D., 2002, *The National Elevation Dataset: Photogrammetric Engineering and Remote Sensing*, v. 68, no. 1, p. 5-11.
- Gibbons, P., R. B. Cunningham, and D. B. Lindenmayer. 2008. What factors influence the collapse of trees retained on logged sites? A case-control study. *Forest Ecology and Management* 255:62-67.
- Gilbertson, R.L., 1980. Wood-rotting fungi of North America. *Mycologia* 72, 1–49.

- Gomez, G., M. Luz Calle, R. Oller and K. Langohr. 2009. Tutorial on methods for interval-censored data and their implementation in R. *Statistical Modelling* 9: 259-297.
- Gonzalez, P., G. P. Asner, J. J. Battles, M. A. Lefsky, K. M. Waring, and M. Palace. 2010. Forest carbon densities and uncertainties from Lidar, QuickBird, and field measurements in California. *Remote Sensing of Environment* 114:1561-1575.
- Harmon, M.E., B. Fasth, C.W. Woodall and J. Sexton. 2013. Carbon concentration of standing and downed woody detritus: effects of tree taxa, decay class, position, and tissue type. *Forest Ecology and Management*. 291: 259-267.
- Harmon, M.E., C. W. Woodall, B. Fasth, J. Sexton and M. Yatkov. 2011. Differences between standing and downed dead tree wood density reduction factors: A comparison across decay classes and tree species. Res. Pap. NRS-15. Newtown Square, PA: U.S. Department of Agriculture, Forest Service, Northern Research Station. 40 p.
- Harmon, M. E., K. Cromack Jr., and B. G. Smith. 1987. Coarse woody debris in mixed-conifer forests, Sequoia National Park, California. *Canadian Journal of Forest Research* 17:1265-1272.
- Harris, N.L., S. Brown, S.C. Hagen, S.S. Saatchi, S. Petrova, W. Salas, M.C. Hansen, P.V. Potapov, and A. Lotsch. 2012. Baseline map of carbon emissions from deforestation in tropical regions. *Science* 336: 1573-1576.
- Heath, L.S., Hansen, M., Smith, J.E., Miles, P.D., Smith, B.W., 2009. Investigation into calculating tree biomass and carbon in the FIADB using a biomass expansion factor approach. In: McWilliams, Will; Moisen, Gretchen; Czaplowski, Ray, comps. *Forest Inventory and Analysis (FIA) Symposium 2008; October 21-23, 2008; Park City, UT. Proc. RMRS-P-56CD*. Fort Collins, CO: U.S. Department of Agriculture, Forest Service, Rocky Mountain Research Station. 26 p.
- Heath, L.S., J. Smith, K. Skog, D. Nowak, and C. W. Woodall. 2011. Managed forest carbon stock and stock-change estimates for the U.S. Greenhouse Gas Inventory, 1990–2008. *Journal of Forestry* 109, 167–173.
- Hicke, J. A., A.J. Meddens, C.D. Allen and C.A. Kolden. 2013. Carbon stocks of trees killed by bark beetles and wildfire in the western United States. *Environmental Research Letters*: 8(3), 035032.
- Hilger, A. B., C. H. Shaw, J. M. Metsaranta, and W. A. Kurz. 2012. Estimation of snag carbon transfer rates by ecozone and lead species for forests in Canada. *Ecological Applications* 22:2078-2090.
- Holmen, S. P. 1990. Height-diameter regression tables from forest inventory at Blodgett Forest Research Station. Unpublished dataset.

- Homer, C., J. Dewitz, J. Fry, M. Coan, N. Hossain, C. Larson, N. Herold, A. McKerrow, J.N. VanDriel, and J. Wickham. 2007. Completion of the 2001 National Land Cover Database for the conterminous United States. *Photogrammetric Engineering and Remote Sensing* 73: 337-341.
- Hudak, A. T., B. C. Bright, and R. E. Kennedy. 2013. Predicting live and dead basal area from LandTrendr variables in beetle-affected forests. *MultiTemp 2013: 7th International Workshop on the Analysis of Multi-temporal Remote Sensing Images*: 1-4.
- Intergovernmental Panel on Climate Change (IPCC). 2006. Agriculture, Forestry, and Other Land Use. In IPCC. National Greenhouse Gas Inventory Guidelines. Institute for Global Environmental Strategies, Hayama, Japan.
- Intergovernmental Panel on Climate Change (IPCC). 2007. Climate change 2007: the physical science basis. In Contribution of Working Group I to the Fourth Assessment Report of the Intergovernmental Panel on Climate Change. S. Solomon, D. Qin, M. Manning, Z. Chen, M. Marquis, Avery, B., Tignor, M. and Miller, H.L. (eds). Cambridge University Press, Cambridge, UK, 996 pp.
- Intergovernmental Panel on Climate Change (IPCC). 2013a. Climate Change 2013: The Physical Science Basis. Twelfth Session of IPCC Working Group I, Stockholm, Sweden. September 27, 2013.
- Intergovernmental Panel on Climate Change (IPCC). 2013b. Supplement to the 2006 IPCC Guidelines on 24 National Greenhouse Gas Inventories: Wetlands. Thirty-Seventh Session of the IPCC, Batumi, Georgia. October 15, 2013.
- Jennings, M.D., D. Faber-Langendoen, O.L. Loucks, R.K. Peet, and D. Roberts. 2009. Standards for associations and alliances of the U.S. National Vegetation Classification. *Ecological Monographs* 79: 173-199.
- R.E. Kennedy, Z. Yang, and W.B. Cohen. 2010. Detecting trends in forest disturbance and recovery using yearly Landsat time series: 1. LandTrendr — Temporal segmentation algorithms. *Remote Sensing of Environment* 114: 2897–2910.
- Keen, F. P. 1955. The rate of natural falling of beetle-killed ponderosa pine snags. *Journal of Forestry* 53(10):720-723.
- Keen, F. P. 1929. How soon do yellow pine snags fall? *Journal of Forestry* 27:735-737.
- Kruys, N., C. Fries, B. G. Jonsson, T. Lamas, and G. Stahl. 1999. Wood inhabiting cryptograms on dead Norway spruce (*Picea abies*) trees in managed Swedish boreal forests. *Canadian Journal of Forest Research*. 29: 178-186.
- Kurz, W. A., C. C. Dymond, G. Stinson, G. J. Rampley, E. T. Neilson, A. L. Carroll, T. Ebata, and L. Safranyik. 2008. Mountain pine beetle and forest carbon feedback to climate change.

Nature 452:987-990.

- Kurz, W. A., C. C. Dymond, T. M. White, G. Stinson, C. H. Shaw, G. J. Rampley, C. Smyth, B. N. Simpson, E. T. Neilson, J. A. Trofymow, J. Metsaranta, and M. J. Apps. 2009. CBM-CFS3: a model of carbon-dynamics in forestry and land-use change implementing IPCC standards. *Ecological Modelling* 220:480–504.
- Krankina, O. N., and M. E. Harmon. 1995. Dynamics of the dead wood carbon pool in northwestern Russian boreal forests. *Water Air and Soil Pollution*. 82: 227–238.
- Lefsky, M.A. 2010. A global forest canopy height map from the Moderate Resolution Imaging Spectroradiometer and the Geoscience Laser Altimeter System. *Geophysical Research Letters* 37: L15401. doi:10.1029/2010GL043622.
- Loveland, T.R., B.C. Reed, J.F. Brown, D.O. Ohlen, Z. Zhu, L. Yang, and J.W. Merchant. 2000. Development of a global land cover characteristics database and IGBP DISCover from 1-km AVHRR data. *International Journal of Remote Sensing* 21: 1303-1330.
- van Mantgem, P. J., and N. L. Stephenson. 2007. Apparent climatically-induced increase of tree mortality rates in a temperate forest. *Ecology Letters* 10:909-916.
- van Mantgem, P. J., N. L. Stephenson, J. C. Byrne, L. D. Daniels, J. F. Franklin, P. Z. Fule, M. E. Harmon, A. J. Larson, J. M. Smith, A. H. Taylor, and T. T. Veblen. 2009. Widespread Increase of Tree Mortality Rates in the Western United States. *Science* 323:521-524.
- McDonald, P. Incense-cedar ... an American wood. 1973. FS-226 October 1973 United States Department of Agriculture Forest Service, Pacific Southwest Forest and Range Experiment Station, Berkeley, California.
- Miles, P.D. and W. B. Smith. 2009. Specific gravity and other properties of wood and bark for 156 tree species found in North America. Res. Note NRS-38. Newtown Square, PA: U.S. Department of Agriculture, Forest Service, Northern Research Station. 35 p.
- Morrison, M. L., and M. G. Raphael. 1993. Modeling the Dynamics of Snags. *Ecological Applications* 3:322-330.
- Moser, S., G. Franco, S. Pittiglio, W. Chou, and D. Cayan. 2009. The Future Is Now: An Update on Climate Change Science Impacts and Response Options for California. California Energy Commission, PIER Energy-Related Environmental Research Program. CEC-500-2008-071.
- Olson, C. M., and J. A. Helms. 1996. Forest growth and stand structure at Blodgett Forest Research Station. In: *Sierra Nevada Ecosystem Project: Final Report to Congress*, vol. III, Centers for Water and Wildland Resources, University of California, Davis, pp. 681–732.

- Panek, J., D. Saah, A. Esperanza, A. Bytnerowicz, W. Fraczek, and R. Cisneros. 2013. Ozone distribution in remote ecologically vulnerable terrain of the southern Sierra Nevada, CA. *Environmental Pollution* 182:343-356.
- Parish, R., J. A. Antos, P. K. Ott, and C. M. Di Lucca. 2010. Snag longevity of Douglas-fir, western hemlock, and western redcedar from permanent sample plots in coastal British Columbia. *Forest Ecology and Management* 259:633-640.
- Pesonen, A., M. Maltamo, and P. Packalèn. 2008. Airborne laser scanning-based prediction of coarse woody debris volumes in a conservation area. *Forest Ecology and Management* 255: 3288-3296.
- R Core Team. 2014. R: A language and environment for statistical computing. R Foundation for Statistical Computing, Vienna, Austria. URL <http://www.R-project.org/>.
- Raphael, M. G., and M. White. 1984. Use of snags by cavity-nesting birds in the Sierra-Nevada. *Wildlife Monographs* 86:1-66.
- Raphael, M. G., and M. L. Morrison. 1987. Decay and Dynamics of Snags in the Sierra Nevada, California. *Forest Science* 33:774-783.
- Rollins, M.G. 2009. LANDFIRE: a nationally consistent vegetation, wildland fire, and fuel assessment. *International Journal of Wildland Fire* 18: 235–249.
- Roy, D.P., Ju, J., Kline, K., Scaramuzza, P.L., Kovalsky, V., Hansen, M.C., Loveland, T.R., Vermote, E.F., Zhang, C., 2010, Web-enabled Landsat Data (WELD): Landsat ETM+ Compositing Mosaics of the Conterminous United States. *Remote Sensing of Environment* 114: 35-49.
- Running S.W., R.R. Nemani, F.A. Heinsch, M. Zhao, M. Reeves, and H. Hashimoto. 2004. A continuous satellite-derived measure of global terrestrial primary production. *BioScience* 54: 547-560.
- Ryan, K.C., and T.S. Opperman. 2013. LANDFIRE – A national vegetation/fuels data base for use in fuels treatment, restoration, and suppression planning. *Forest Ecology and Management* 294: 208-216.
- Saatchi, S.S., N.L. Harris, S. Brown, M. Lefsky, E.T.A. Mitchard, W. Salas, B.R. Zutta, W. Buermann, S.L. Lewis, S. Hagen, S. Petrova, L. White, M. Silman, and A. Morel. 2011. Benchmark map of forest carbon stocks in tropical regions across three continents. *Proceedings of the National Academy of Sciences of the USA* 108: 9899-9904.
- Schurr, F., 2005. Incense cedar growth studies and observed mortality at Blodgett Forest Research Station. Presentation to the California Forest Pest Council, November 2005. Available at <http://caforestpestcouncil.org/2008/07/2005-cfpc-annual-meeting-online->

proceedings/

- Smith, J. E., L. S. Heath, and J. C. Jenkins. 2003. Forest Volume-to-Biomass Models and Estimates of Mass for Live and Standing Dead Trees of U.S. Forests. General Technical Report NE-298. US Department of Agriculture, Forest Service. Northeastern Research Station, Newtown Square, PA, 57 pp.
- Sokal, R.B. and F. J. Rohlf. 1995. Biometry: The Principles and Practices of Statistics in Biological Research, 3<sup>rd</sup> edition. W.H. Freeman and Company. New York. 850p.
- Spears, J. D., S. M. Holub, M. E. Harmon, and K. Lajtha. 2003. The influence of decomposing logs on soil biology and nutrient cycling in an old-growth mixed coniferous forest in Oregon, U.S.A. *Canadian Journal of Forest Research* 33:2193-2201.
- Stephens, S.L., J.K. Agee, P.Z. Fulé, M.P. North, W.H. Romme, and T.W. Swetnam, 2013. Managing forests and fire in changing climates. *Science* 342: 41–42.
- Thomas, J. W. 1979. Wildlife Habitats in Managed Forests of the Blue Mountains of Oregon and Washington (Agriculture Handbook No. 553). September 1979. USDA Forest Service.
- Thomas, J. W., (technical editor) 1979. Wildlife habitats in managed forests of the Blue Mountains of Oregon and Washington. USDA-Forest Service Agriculture Handbook Number 553. Published in cooperation with the Wildlife Management Institute Washington, D.C. and the U.S. Department of Interior Bureau of Land Management.
- Tucker, C.J. 1979. Red and photographic infrared linear combinations for monitoring vegetation. *Remote Sensing of Environment* 8: 127-150.
- Tucker, C.J., C.L. Vanpraet, M.J. Sharman, and G. Van Ittersum. 1985. Satellite remote sensing of total herbaceous biomass production in the Senegalese Sahel: 1980–1984. *Remote Sensing of Environment* 17: 233-249.
- Turnbull, B.W. 1976. The empirical distribution function with arbitrarily grouped, censored and truncated data. *Journal of the Royal Statistical Society B* 38: 290-295.
- Turner, D.P., W.D. Ritts, W.B. Cohen, S.T. Gower, S.W. Running, M. Zhao, M.H. Costa, A. Kirschbaum, J. Ham, S. Saleska, and D.E. Ahl. 2006. Evaluation of MODIS NPP and GPP products across multiple biomes. *Remote Sensing of Environment* 102: 282-292.
- United Nations, 1992. UN General Assembly, United Nations Framework Convention on Climate Change : resolution / adopted by the General Assembly, 20 January 1994, A/RES/48/189, Available online:  
[http://unfccc.int/essential\\_background/convention/background/items/1353.php](http://unfccc.int/essential_background/convention/background/items/1353.php)
- U.S. Environmental Protection Agency (EPA). 2011. Inventory of U.S greenhouse gas emissions

and sinks: 1990-2009. USEPA; 430-R-11-005.

United States Department of Agriculture - Forest Service (USDA-FS), 2010. Forest Inventory and Analysis national core field guide Volume 1: field data collection procedures for phase 2 plots, version 5.0. Available: <http://www.fia.fs.fed.us/library/field-guides-methods-proc/docs/Complete%20FG%20Document/NRS%20FG%205.0-Oct%202010-Complete%20Document.pdf>

United States Department of Agriculture - Forest Service (USDA-FS), 2013. Baseline assessment of forest carbon stocks including harvested wood products – USDA Forest Service, Pacific Southwest Region. Report from the Climate Change Advisor’s Office, Office of the Chief.

United States Department of the Interior, Geological Survey (USGS-LANDFIRE), 2008. LANDFIRE: LANDFIRE 1.1.0 Existing Vegetation Type layer. [Online]. Available: <http://landfire.cr.usgs.gov/viewer/>

Vanderwel, M.C., Thorpe, H.C., Shuter, J.L., Caspersen, J.P., Thomas, S.C., 2008. Contrasting downed woody debris dynamics in managed and unmanaged northern hardwood stands. *Canadian Journal of Forest Research* 38, 2850-2861.

Williamson, G. B., and M. C. Wiemann. 2010. Measuring Wood Specific Gravity ... Correctly. *American Journal of Botany* 97:519-524.

Wensel, L. C., and C. M. Olson. 1995. Tree taper model volume equations. *Hilgardia* 62, December 1995.

Whittaker, R. H., G. E. Likens, F. H. Bormann, J. S. Easton, and T. G. Siccama 1979. The Hubbard Brook Ecosystem Study: Forest Nutrient Cycling and Element Behavior. *Ecology* 60:203–220. <http://dx.doi.org/10.2307/1936481>

Whittaker, R. H.; Woodwell, G. M. 1968. Dimension and production relations of trees and shrubs in the Brookhaven Forest, New York. *Journal of Ecology*. 56(1): 1-25.

Woodall, C.W., L. S. Heath, G. M. Domke and M. C. Nichols. 2011. Methods and equations for estimating aboveground volume, biomass, and carbon for trees in the U.S forest inventory, 2010. Gen Tech Rep NRS-88 USDA Forest Service, Northern Research Station.

Woodall, C.W., G.M. Domke, D.W. MacFarlane and C.M. Oswalt. 2012. Comparing field- and model-based standing dead tree carbon stock estimates across forests of the US. *Forestry*. 85: 125-133.

Woodall, C. W.; Waddell, K. L.; Oswalt, C. M.; Smith, J. E. 2013. Standing dead tree resources in forests of the United States. In: Potter, Kevin M.; Conkling, Barbara L., eds. 2013. *Forest Health Monitoring: national status, trends, and analysis 2010*. Gen. Tech. Rep. SRS-GTR-176.

Asheville, NC: U.S. Department of Agriculture Forest Service, Southern Research Station.  
85-94

Woudenberg S. W., B. L. Conkling, B. M. O'Connell, E. B. LaPoint, J. A Turner, and K. L. Waddell. 2010. The Forest Inventory and Analysis Database: Database description and users manual version 4.0 for Phase 2. Gen Tech Rep RMRS-GTR-245 USDA Forest Service, Rocky Mountain Research Station. Available at <http://www.fia.fs.fed.us/library/database-documentation/>

Zheng, D. L. S. Heath, M.J. Ducey and J. E. Smith. 2011. Carbon changes in conterminous US forests associated with growth and major disturbances: 1992–2001. *Environmental Resource Letters* 6: 014012.

Zolkos, S. G., S. J. Goetz, and R. Dubayah. 2013. A meta-analysis of terrestrial aboveground biomass estimation using lidar remote sensing. *Remote Sensing of Environment* 128: 289-298.